Journal of Medicinal Chemistry

pubs.acs.org/jmc

Drug Annotation

Discovery of Encequidar, First-in-Class Intestine Specific P-glycoprotein Inhibitor

Michael P. Smolinski,* Sameer Urgaonkar, Laura Pitzonka, Murray Cutler, GwanSun Lee, Kwee Hyun Suh, and Johnson Y. N. Lau

Cite This: *J. Med. Chem.* 2021, 64, 3677−3693

Read Online

ACCESS | Metrics & More | Article Recommendations | Supporting Information

ABSTRACT: Many chemotherapeutics, such as paclitaxel, are administered intravenously as they suffer from poor oral bioavailability, partly because of efflux mechanism of P-glycoprotein in the intestinal epithelium. To date, no drug has been approved by the U.S. Food and Drug Administration (FDA) that selectively blocks this efflux pump. We sought to identify a compound that selectively inhibits P-glycoprotein in the gastrointestinal mucosa with poor oral bioavailability, thus eliminating the issues such as bone marrow toxicity associated with systemic inhibition of P-glycoprotein. Here, we describe the discovery of highly potent, selective, and poorly orally bioavailable P-glycoprotein inhibitor **14** (encequidar). Clinically, encequidar was found to be well tolerated and minimally absorbed; and importantly, it enabled the oral delivery of paclitaxel.

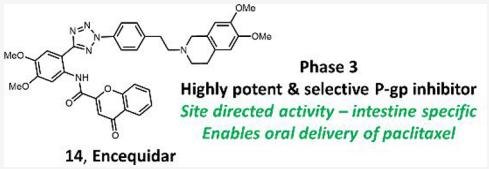

INTRODUCTION

P-glycoprotein (P-gp), a 170 kDa membrane protein encoded by the *mdr1* gene in humans and belonging to the class of ABC (ATP-binding cassette) transporters, was identified by Victor Ling in 1976 as a permeability alteration protein in colchicine-resistant Chinese hamster ovary cells.[1,2] Since then, P-gp has shown to be expressed in various healthy and malignant tissues where it serves a diversity of functions.[3−6] The presence of P-gp on the apical surface of epithelial cells of the small intestine promotes the efflux of both endogenous and xenobiotic substrates. Similarly, localization of P-gp on the biliary canalicular membrane of hepatocytes and on the epithelial cells of proximal convoluted tubules of nephrons facilitates biliary and renal excretion of its substrates, respectively. Its existence in the endothelial cells of the blood-brain barrier provides protection to the brain against circulating toxins in the blood. Moreover, overexpression of P-gp in cancer cells is associated with drug resistance phenotype compromising the efficacy of anticancer drugs which are substrates of P-gp.[7−9]

Oral dosing is a preferred route of administration,[10] more so during a global pandemic, for patients due to ease of administration and reduction in hospital/clinic visits. The oral route enables development of novel dosing regimens, such as metronomic, and expands treatment options when used alone or in combination with other anticancer drugs. One of the most widely used classes of chemotherapeutic drugs, taxanes, such as paclitaxel and docetaxel, are administered intravenously as they suffer from poor oral bioavailability.[11] While providing transformative tumor shrinkage, these drugs are formulated in vehicles containing nonionic surfactants such as polyoxyl-35 castor oil (for paclitaxel) and tween 80 (for docetaxel) to allow them to be administered intravenously. Clinically, systemic exposure of these excipients can result in serious side effects such as hypersensitivity reactions, hyperlipidemia, sometimes irreversible sensory neuropathy, and cumulative fluid retention.[12] To reduce these risks, often patients are premedicated with corticosteroids and antihistamines. Oral administration of these drugs is expected to eliminate or significantly reduce these side effects without necessitating the use of premedications.

The poor oral absorption of paclitaxel and docetaxel can be attributed to three important underlying factors: (a) when given orally these drugs are recognized by P-gp in the intestinal cells of the gastrointestinal tract and undergo drug efflux back out into the intestinal lumen; (b) these drugs have poor aqueous solubility, and (c) these drugs undergo cytochrome P450-mediated (specifically CYP3A4/5) intestinal metabolism.[13] Because of the direct role of intestinal P-gp in oral absorption, it has been the subject of much interest as a target for boosting oral bioavailability of substrates of P-gp. One of the early papers describing the potential of intestinal P-gp in oral bioavailability enhancement of a substrate drug appeared in 1993 wherein quinidine was used as a P-gp inhibitor to improve the absorption of etoposide, a P-gp substrate, in rats.[14] This finding led to a renaissance in the development of inhibitors targeting P-gp.

Received: December 4, 2020
Published: March 17, 2021

https://doi.org/10.1021/acs.jmedchem.0c01826
J. Med. Chem. 2021, 64, 3677−3693

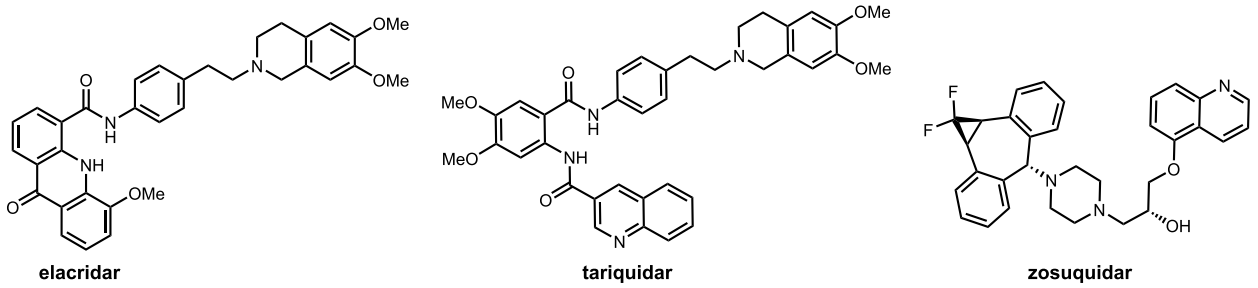

Figure 1. Representative structures of third generation P-gp inhibitors.

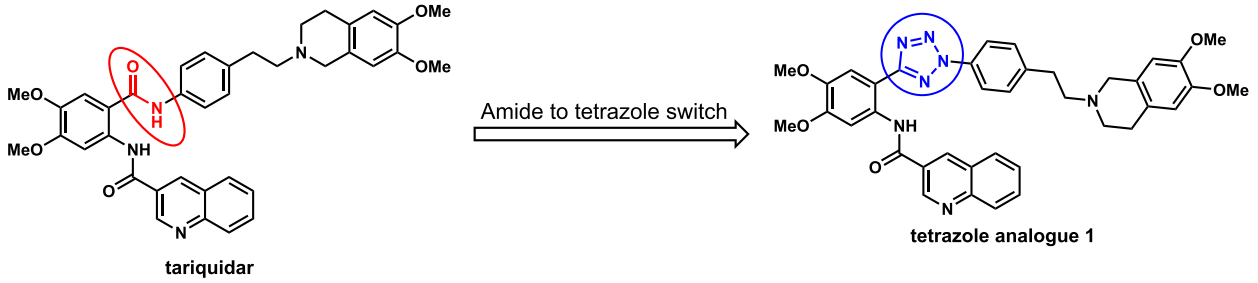

Figure 2. Layout of structural modification proposed to limit the systemic absorption of P-gp inhibitor tariquidar.

The discovery of first-generation P-gp inhibitors was serendipitous and included the calcium channel blocker verapamil and the immunosuppressive agent cyclosporin A.[15] Particularly, the use of oral cyclosporin A, in the landmark proof of concept study conducted by Terwogt and co-workers,[16,17] improved the oral bioavailability of paclitaxel up to 10-fold (47% versus 4% without cyclosporin A) in a clinical setting. This study clinically validated intestinal P-gp as a target for improving oral bioavailability of paclitaxel.

Paclitaxel, a well characterized P-gp substrate, is listed by the World Health Organization (WHO) as an essential medicine for the treatment of cancer. Remarkably, since its approval by the U.S. Food and Drug Administration (FDA) in 1992 for ovarian cancer, it has grown leaps and bounds and has been established as one of the mainstay drugs in the fight against cancer. While paclitaxel is administered intravenously either as Taxol or as nanoparticle albumin-bound paclitaxel, also known as *nab*-paclitaxel (Abraxane), transforming this mode of administration into oral has remained a challenge in the oncology community. However, the breakthrough result discussed above paved the path to discover a more selective P-gp inhibitor suitable for facilitating the oral absorption of P-gp substrates, such as paclitaxel.

The initial promising result with cyclosporin A was tempered knowing that the original intended pharmacology of cyclosporin A being immunosuppressive was undesirable in a paclitaxel-based cancer treatment regimen, as this could compromise the immune system when needed most. Second-generation P-gp inhibitors, for example, dexverapamil (the less potent calcium antagonist *R*-enantiomer of verapamil)[18] and valspodar[19,20] (a nonimmunosuppressive derivative of cyclosporin A), provided compounds with P-gp inhibition but lacked selectivity among transporters and metabolic enzymes. The potential drug−drug interactions of these less selective P-gp inhibitors would significantly complicate their use with paclitaxel to facilitate oral absorption.[21,22] Third-generation P-gp inhibitors, such as elacridar[23,24] (GF120918), tariquidar[25] (XR9576), OC144-093[26,27] (ONT-093), zosuquidar[28,29] (LY335979), and laniquidar[30,31] (R101933) have excellent potency against P-gp and demonstrated selectivity; however, they were developed primarily for combatting P-gp-mediated cancer drug resistance and were orally bioavailable with significant systemic exposure (Figure 1). Not surprisingly, many of the adverse events recorded for these P-gp inhibitors, following administration of P-gp substrate anticancer drugs (for example, paclitaxel), were due to on-target systemic P-gp inhibition in sensitive tissues, including the bone marrow and the central nervous system (CNS), resulting in an increased exposure of these tissues to the anticancer drug leading to augmented toxicity.

In our quest to develop a novel P-gp inhibitor to improve the oral bioavailability of its substrate drugs including taxanes, we reasoned that specific targeting of intestinal P-gp by a selective small molecule inhibitor with low systemic exposure would represent an attractive approach. A tissue and target specific inhibitor would have the potential to improve oral bioavailability of a substrate drug while avoiding undesirable metabolism[21] or clearance[22] of substrate drugs that may exacerbate side effects. This approach of ours, if successful and safe, could serve as a platform technology allowing for oral absorption of several drugs with P-gp mediated efflux liability.[32] In this drug annotation paper, we describe our journey of bringing an intestine specific P-gp inhibitor, encequidar, from conception to the clinic.

RESULTS AND DISCUSSION

Discovery of Encequidar. Our drug discovery strategy entailed identifying a compound with the following attributes: (a) high selectivity and potency for P-gp, (b) poor systemic absorption, and (c) ability to improve the oral bioavailability of P-gp substrates, such as paclitaxel. At the onset, it was apparent that several conventional rules dictating physicochemical properties desired in an orally bioavailable drug, such as MW < 500, log *P* < 5, HBD < 5, HBA < 10, *i.e.*, Lipinski's rule of 5 (Ro5),[33] would need to be violated in successfully designing an inhibitor that is restricted to the gastrointestinal tract. P-gp is a

https://doi.org/10.1021/acs.jmedchem.0c01826
J. Med. Chem. 2021, 64, 3677−3693

Table 1. SAR Optimization of Tetrazole Series

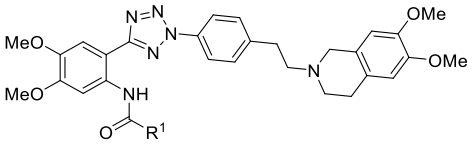

compound	R^1	P-gp[a] EC_{50} (nM)	paclitaxel EC_{50} (nM) cell lines		paclitaxel cytotoxicity enhancement[b]
			MCF-7	MCF-7/Dox	
tariquidar		16	-	-	-
control			11.5	294.6	1.0
1		75	7.9	14.5	20.3
2		-	12.1	109.9	2.7
3		-	8.5	83.8	3.5
4		-	5.4	69.2	4.3
5		-	7.6	162.0	1.8
6		-	9.1	88.6	3.3
7		-	9.1	97.9	3.0
8		-	10.3	112.7	2.6
9		-	9.1	97.9	3.0

compound	R^1	P-gp[a] EC_{50} (nM)	paclitaxel EC_{50} (nM) cell lines		paclitaxel cytotoxicity enhancement[b]
			MCF-7	MCF-7/Dox	
10		-	7.7	86.9	3.4
11		-	10.3	80.4	3.7
12		-	6.4	66.2	4.5
13		-	10.2	83.7	3.5
14	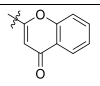	13	7.9	4.9	60.1
15	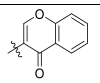	-	9.0	139.5	2.1
16	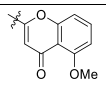	-	7.4	5.9	49.9
17	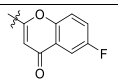	-	8.1	7.5	39.3
18	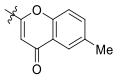	-	6.5	4.0	73.4

[a]P-gp activity was measured via a cell growth inhibition assay with 200 nM paclitaxel in MES-SA/DX5, a P-gp overexpressing cell line, by varying the concentrations of the P-gp inhibitor. While 200 nM paclitaxel inhibited 100% cell growth in the parental cell line MES-SA, this concentration of paclitaxel showed minimal inhibition in MES-SA/DX5. [b]Paclitaxel cytotoxicity enhancement represents the ratio of paclitaxel EC_{50}'s in MCF7/Dox (drug-resistant cell line) in the absence (control) and in the presence of an inhibitor (50 nM) with higher values corresponding to greater P-gp inhibition by an inhibitor.

transmembrane protein, expressed on the apical side of polarized enterocytes lining the walls of the small intestine, a major site for absorption of small molecules into the bloodstream (systemic absorption). For an inhibitor of P-gp to have a pharmacological effect, it has to either cross the upper leaflet of a lipid bilayer and bind to the internal cavity of P-gp or travel across the bilayer to the cytosolic end to enter the drug binding domain in the transmembrane region or bind to the nucleotide binding domain.[34−38] In either case, maintaining a balance between cellular permeability and absorption would be critical in designing a site-specific P-gp inhibitor.

To realize our goal, we turned our focus on tariquidar, a highly potent P-gp inhibitor first reported by researchers at Xenova Group Ltd. in 1999,[39] for medicinal chemistry optimization (Figure 2). Structurally, tariquidar possesses a tetrahydroisoquinoline ring connected via a hydrophobic linker to an anthranilamide portion equipped with a hydrophobic heterocyclic ring. The extensive structure−activity relationship (SAR) of tariquidar clearly established the importance of tetrahydroisoquinoline ring as well as the lower amide bond linked to quinoline for P-gp inhibitory potency.[40,41] Despite the high molecular weight, tariquidar is surprisingly orally bioavailable.[42] To understand factor(s) influencing tariquidar's oral bioavailability, and which could be manipulated using medicinal chemistry strategies, we looked at its Ro5 parameters and recognized them to be mostly on the anomalous side with regard to the Lipinski rules, considered gold standard for oral drugs. However, one of the key molecular descriptors beyond Ro5, the topological polar surface area (tPSA) of tariquidar of 111.26 $Å^2$, falls well within the limit of 140 $Å^2$ set for well absorbed drugs.[43−45] Notably, another orally absorbed P-gp inhibitor elacridar[46] follows a similar pattern as tariquidar and has a tPSA of 92.90 $Å^2$.

Because tPSA is a high throughput molecular descriptor accounting for polar 2D fragments in a molecule and has shown to have good correlation with cellular permeability and oral absorption[47] we employed this parameter as a guiding tool

https://doi.org/10.1021/acs.jmedchem.0c01826
J. Med. Chem. 2021, 64, 3677−3693

Scheme 1. Synthesis of Encequidar (14)[a]

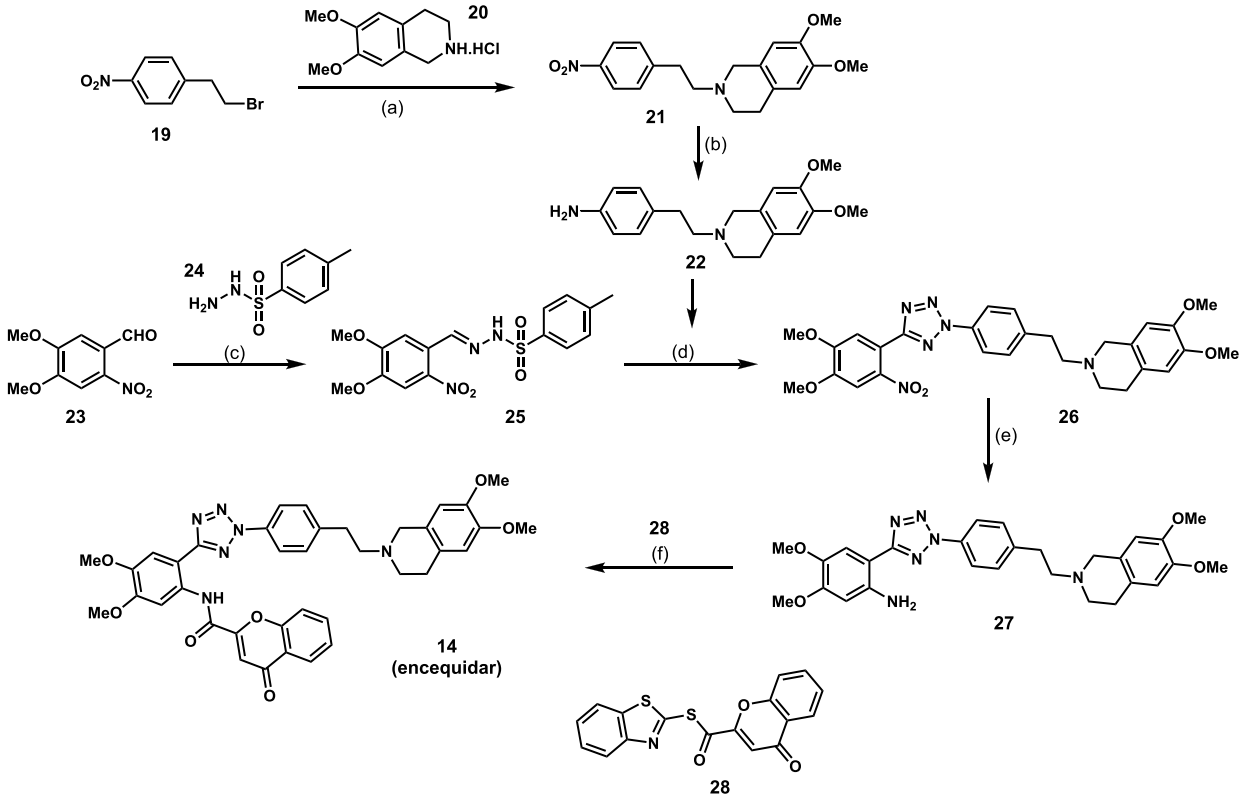

[a]Reagents and conditions: (a) **20**, K_2CO_3, NaI, DMF, 100 °C; (b) H_2, Pd/C, THF-MeOH (1:1), 68% yield over two steps; (c) EtOH, **24**, 80 °C, 85% yield; (d) **22**, $NaNO_2$, conc. HCl, EtOH, H_2O, −15 °C then **25**, pyridine, 70% yield; (e) H_2, Pd/C, EtOH-DCM (1:1), 85% yield; (f) **28**, DCM, rt, 72% yield.

for designing poorly orally bioavailable P-gp inhibitors. We sought to do subtle but unique modifications in the tariquidar structure to further increase the tPSA and thereby reduce the oral absorption.

Conformationally restrained tetrazoles are well-known bioisosteres for amides in peptide and medicinal chemistry.[48,49] Tetrazoles possess several key traits. First, this structural moiety increases the tPSA without having a deleterious effect on lipophilicity. Second, all four nitrogen atoms of tetrazole can theoretically participate in hydrogen bond interactions with the active site residues of a protein (P-gp in the present context) and therefore have the potential to supplement interactions offered by the amide group. On the other hand, although not definitive, the SAR studies of tariquidar suggest the importance of the upper amide group for P-gp potency.[39] Thus, loss of this amide group (and its hydrogen bond acceptor and donor features) could potentially diminish any advantage offered by the isosteric replacement with tetrazole. Finally, tetrazoles tend to be metabolically more stable than the amides, a desirable characteristic to provide adequate exposure in the intestine, an organ with significant metabolic capacity.[50] It is worth noting here that, despite the increased stability, we anticipated that the tetrazole scaffold would negatively impact permeability across enterocytes, the absorptive cells of the intestine, and into the bloodstream due to a significant increase in tPSA. All these remarkable features presented by tetrazole led us to explore this heterocycle as a replacement of the amide bond of tariquidar while keeping the tetrahydroisoquinoline nucleus as well as the hydrophobic lower amide intact.

The subtle architectural modification of tariquidar was rapidly accomplished and provided the tetrazole analogue **1**. Encouragingly, this bioisosteric switch of amide group with tetrazole ring retained the capacity to inhibit the P-gp activity although with diminished potency as compared to tariquidar (Table 1). Nevertheless, this result undermines the notion that the hydrogen bond donor of the amide group would be necessary for P-gp activity. Alternatively, the polar interactions of the four nitrogen atoms with the P-gp binding site compensate for any loss in activity due to the absence of the hydrogen bond donor group in the tetrazole analogue. Furthermore, tetrazole **1** had a larger tPSA of 125.77 $Å^2$ and a reduced lipophilicity of 5.02 (cLogP) as compared with tariquidar (tPSA of 111.26 $Å^2$ and cLogP of 5.55). Having obtained this promising result, we set out to further improve the potency and increase the tPSA in our pursuit for a clinical candidate with a poor absorption profile.

Next, we put our efforts in exploring the hydrophobic core of the lower amide portion. As can be seen from the examples presented in Table 1, the SAR around the quinoline group was quite narrow and clearly favored fused (bicyclic) heterocycles.[51] Thus, phenyl, naphthalene, as well as various substituted aromatics as replacements for the quinoline group resulted in a considerably reduced P-gp inhibitory activity. Even nonfused heterocycles including pyridines, thiophene, and furan were not tolerated in lieu of quinoline. Notably, the position of the heteroatom (nitrogen) in the heterocycle was also found to be equally important, with at least one nitrogen atom *meta* to the amide carbonyl proving vital for increased potency. These unique structural require-

https://doi.org/10.1021/acs.jmedchem.0c01826
J. Med. Chem. 2021, 64, 3677−3693

ments of a fused heterocycle and the heteroatom position indicate that favorable $\pi-\pi$ interactions (and hydrogen bonding) may be at play.

Replacement of nitrogen-based heterocycle with chromone had the greatest overall impact on improving the potency of this series. Not only the choice of this heterocycle but also the position of chromone carbonyl with respect to the amide carbonyl had a profound impact on the P-gp potency displayed by these inhibitors. Thus, tetrazole **14** with chromone carbonyl positioned *meta* to the amide carbonyl was found to be to be an equally potent inhibitor of P-gp as tariquidar and emerged as the leading candidate with 5-fold improvement in the P-gp activity over the quinoline tetrazole **1** (Table 1). Surprisingly, this gain in potency was completely negated when the chromone carbonyl was *ortho* to the amide carbonyl as in the tetrazole analogue **15**. Next, the SAR exploration focused around the chromone ring led us to synthesize tetrazole analogues **16**–**18** with a monosubstituted chromone ring. Except for tetrazole analogue **18**, which contained the Me substituted chromone, substitutions at the chromone ring did not improve the potency as compared to **14**. The greater potency of chromone-derived tetrazole analogues as compared to the quinoline derived tetrazoles suggests that the chromone is especially well suited to engage in key interactions with P-gp. Although tetrazole analogue **18** demonstrated greater *in vitro* potency than **14**, it was not pursued further because it was deemed that an extra methyl group of **18** could be metabolically labile *in vivo*.

Excellent *in vitro* potency coupled with poor permeability and aqueous solubility (Table 2) prompted us to evaluate tetrazole **14** (INN-encequidar) in a rat pharmacokinetic study with the anticipation that these favorable physicochemical properties would translate into poor oral bioavailability *in vivo*.[52] The results are discussed in the preclinical pharmacokinetics section.

Chemistry. The synthesis of encequidar (**14**) was performed as described in Scheme 1.[51] Two key building blocks, compounds **22** and **25**, were first constructed using commercially available starting materials via straightforward chemistry. The key tetrazole ring forming reaction from **22** and **25** proceeded smoothly, as described by Kondo et al.,[53] to afford **26**. Reduction of the nitro group in **26** followed by coupling of resultant aniline **27** with the thioester **28**, readily synthesized from chromone-2-carboxylic acid, afforded **14** (encequidar). The synthetic route to other final tetrazoles is analogous to **14** except for the last step where the aniline **27** was either coupled with the carboxylic acids using EDCI/cat.DMAP or with the thioesters derived from the corresponding carboxylic acids.[51]

Encequidar vs Third Generation P-gp Inhibitors—Differences in Physicochemical Properties. Next, we examined key physicochemical parameters, generally attributed to oral bioavailability, for the third-generation P-gp inhibitors and compared them with encequidar to justify our selection of encequidar for further investigation. The details are presented in Table 2. As can be seen, metrics that clearly stand out for encequidar are molecular weight combined with tPSA, and total hydrogen bond number, all highest among the P-gp inhibitors surveyed. Thus, the increase in polarity that results from large tPSA and hydrogen bond count could be associated with extensive solvation of encequidar in the intestinal lumen aqueous environment and any passive permeability across the lipid bilayer would come at the expense of a very large desolvation penalty. It is to be noted that the possibility of intramolecular hydrogen bond formation in tariquidar, elacridar, and encequidar could offer an opposing effect of increased cellular permeability. We next assessed the passive permeability of all four inhibitors in MDCKII (Madin-Darby canine kidney) cells. While none of the inhibitors tested exhibited good permeability in the traditional sense for orally bioavailable compounds, extremely poor permeability of encequidar of at least 2 orders of magnitude less than the other third generation P-gp inhibitors was striking.

Table 2. Comparison of Physicochemical Properties of Encequidar and Third Generation P-gp Inhibitors

	tariquidar	elacridar	zosuquidar	encequidar
molecular weight	646.7	563.6	527.6	688.7
tPSA (Å^2)[a]	111.26	92.90	48.83	143.09
cLogP[b]	5.55	4.21	4.96	3.99
hydrogen bond donor number	2	2	1	1
hydrogen bond acceptor number	10	8	7	13
MDCKII permeability (3 μM) A→B, P_{app} ($\times 10^{-5}$ cm/s)	0.11	0.01	0.11	0.0002
rotatable bond number	11	8	6	11
aqueous solubility (μg/mL)	2500[c]	0.123[d]	nd[e]	0.219[f]

[a]Calculated using Molinspiration Software.[54] [b]Calculated using ChemDraw Professional 15.1 (PerkinElmer). [c]At pH 5.5.[55] [d]Neutral pH.[56] [e]nd = not determined. [f]At pH 3.8.

Another variable implicated in the poor oral bioavailability is the molecular flexibility[45] as measured by the number of rotatable bonds which were 11, 8, 6, and 11 for tariquidar, elacridar, zosuquidar, and encequidar, respectively (assuming no intramolecular hydrogen bonding). Again, encequidar (and tariquidar) is above the limit set for number for rotatable bonds ($\leq$10) in a drug for good oral bioavailability. Overall, the combination of poor cellular permeability and very low aqueous solubility (desirable features in the present context) boded well for continued development of encequidar as P-gp inhibitor with poor systemic absorption potential.

Pharmacology. *Mechanism of Action.* P-gp as a primary molecular target of encequidar was validated by Li et al. using affinity-based protein profiling combined with the quantitative proteomics approach of SILAC (stable isotope labeling with amino acids in cell culture).[57] Furthermore, bioimaging experiments in either paclitaxel-resistant HT1080 cells[58] or doxorubicin-resistant HepG2 cells[57] using fluorescently labeled encequidar probes established that encequidar colocalizes with P-gp in the cellular membrane, perinuclear space, and endoplasmic reticulum.

Molecular Docking Studies. Recent advances in the structural biology have led to determination of cryo-electron microscopy (EM) structures of human P-gp bound to its substrate, paclitaxel (3.6 Å resolution), and human-mouse chimeric P-gp bound to its inhibitor, zosuquidar (3.9 Å resolution).[59−63] These structures have contributed to our understanding of how a substrate and an inhibitor bind to P-gp. As revealed by these structures, a highly dynamic P-gp encompasses large internal binding pocket surrounded by transmembrane helices within the lipid bilayer. Both the substrate (paclitaxel) and the inhibitor (zosuquidar) occupy a similar region within this pocket sharing some of the binding

https://doi.org/10.1021/acs.jmedchem.0c01826
J. Med. Chem. 2021, 64, 3677−3693

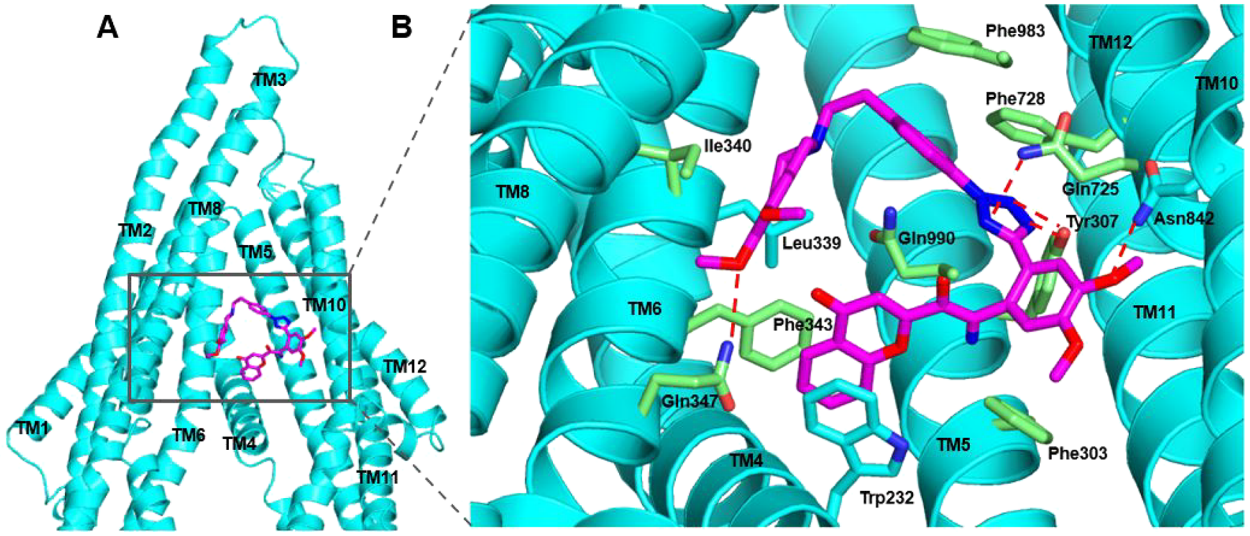

Figure 3. Predicted binding mode of encequidar. A 3D representation of human P-gp (PDB code 6QEX) docked with encequidar is shown as a cartoon with transmembrane domain 1 and 2 helices colored in cyan. Alpha helices 7 and 9, and nucleotide binding domains 1 and 2 are not shown for clarity. (A) Top ranked binding pose of encequidar (shown as magenta stick model). (B) Close-up view of of active site of encequidar surrounded by key amino acid residues of human P-gp. Red dashed lines represent hydrogen bonds. The figures were generated using PyMol and Microsoft Powerpoint. Color code for amino acid residues: C_{flex}, green; C_{rigid}, cyan; N, blue; O, red. Color code for encequidar: C, magenta; N, blue; O, red.

residues. We performed flexible molecular docking studies[64] using the cryo-EM structure of paclitaxel-bound human P-gp (PDB code 6QEX) to retrospectively understand the plausible binding interactions contributing to encequidar's potency. Encequidar was docked into the M-site (modulator site) where other P-gp inhibitors such as zosuquidar[59] and cyclic peptide inhibitors QZ59-*RRR* and QZ59-*SSS*[63] are known to bind. According to our docking results, presented in Figure 3, the binding affinity for the top 10 binding poses of encequidar ranged from −12.5 to −11.9 kcal mol^{-1}. As per the most favorable docked pose, encequidar is oriented in the U-shaped conformation. The chromone ring is sandwiched between aromatic rings of Trp232 and Phe343, making $\pi-\pi$ stacking interactions. The tetrazole ring partakes in hydrogen-bond interactions with Gln725 and Tyr307 and is also involved in $\pi-\pi$ interactions with Phe728. The tetrahydroisoquionline core is mostly surrounded by hydrophobic amino acid residues such as Ile340, Leu339, and Phe343. Two additional hydrogen-bond interactions were predicted for two of the four methoxy groups with Asn842 and Gln347. Collectively, the docking model predicts that encequidar interacts strongly with the M-site located in the deep inner cavity of the transmembrane region of P-gp. Tariquidar was also found to dock favorably in this region with the top pose adopting a U-shape conformation (binding affinities ranged from −12.2 to −11.4 kcal mol^{-1}, data not shown), correlating well with our experimental results and consistent with the binding site predictions for tariquidar made by McCormick et al.[65] and Ferreira et al.[66] via docking studies and by Loo and Clarke[67a] through cysteine cross-linking and arginine mutagenesis studies. Interestingly, the U-shape conformation of tariquidar was also predicted using 3D-QSAR analysis by Labrie et al.[67b]

Selectivity. Previously published studies showed encequidar is a potent and selective P-gp inhibitor, both main goals of the medicinal chemistry program.[52] Because ATP hydrolysis drives the excretory function of P-gp, we examined encequidar's effect on the ATPase activity of P-gp. In an ATPase assay using MDR1 (P-gp)-enriched vesicles, encequidar inhibited P-gp with high potency (IC_{50} = 0.6 nM) and was more potent than known P-gp inhibitors tested (cyclosporin A, tariquidar, and elacridar). Encequidar also showed high specificity for P-gp and did not inhibit the ATPase activity of other ABC transporters tested, MRP1, MRP2, MRP3, or BCRP (Table 3).

Table 3. *In Vitro* ABC Transporter Selectivity Data for Encequidar

	inhibition of ATPase activity, IC_{50} (nM)[a]			
ABC transporter	encequidar	elacridar	tariquidar	cyclosporin A
P-gp	0.6	4.9	32.7	141.3
BCRP	>3717	252.2	183.3	>6568
MRP1	>27 233	>4128	23 780	1412
MRP2	>100 000			16 270
MRP3	>100 000			631.5

[a]ATPase assay using transporter enriched membrane vesicles. Activators: paclitaxel (0.05 μM) for P-gp, sulfasalazine (10 μM) for BCRP, NEM-GS (3 mM) with GSH (2 mM) for MRP1, sulfasalazine (150 μM) with GSH (2 mM) for MRP2, benzmarone (50 μM) with GSH (2 mM) for MRP3. Adapted with permission from ref 52. Copyright 2010 Elsevier.

In a more recent study, the *in vitro* interaction potential between encequidar and the human bile salt export pump (BSEP) efflux transporter and human MATE1, MATE2-K, OAT1, OAT3, OATP1B1, OATP1B3, OCT1, and OCT2 transporters from the solute carrier (SLC) superfamily was evaluated to further explore the selectivity of encequidar. Vesicular transport assays were used to evaluate BSEP, and cellular uptake and inhibition assays were used to evaluate the SLC carriers. BSEP-expressing membrane vesicles and corresponding empty inside-out membrane vesicles were used in the vesicular transport assays, while Chinese hamster ovary, HEK293, and MDCKII cells stably expressing the respective SLC transporters and the corresponding controls

https://doi.org/10.1021/acs.jmedchem.0c01826
J. Med. Chem. 2021, 64, 3677−3693

were used in the cellular uptake and inhibition assays. In these assays, encequidar showed no inhibition on BSEP at concentrations of up to 10 μM and <50% inhibition on MATE1, MATE2-K, OAT1, OAT3, OATP1B1, OATP1B3, OCT1, and OCT2 transporters at concentrations of up to 100 μM. Additionally, encequidar did not inhibit any of the major human cytochrome P450 isoforms (CYP1A2, CYP2A6, CYP2C8, CYP2C9, CYP2C19, CYP2D6, and CYP3A4/5) at concentrations up to 50 μM or induce CYP1A2, CYP2B6, and CYP3A4 at concentrations up to 1 μM.

Together, the *in vitro* transporter and metabolic enzyme data highlight a key advantage of the encequidar molecule, its selectivity. Regulatory authorities, such as the FDA and EMA (European Medicines Agency), require *in vitro* studies to evaluate the interaction potential between investigational drugs and transporters to help evaluate the risk of the investigational drug causing potentially dangerous drug−drug interactions. Therefore, these data provide valuable safety information for the development of encequidar, as we have shown low drug interaction potential for encequidar based transporter activity, beyond its intestine specific pharmacological action on P-gp following oral dosing.

Inhibition of P-gp-Mediated Intestinal Efflux of Paclitaxel. Since encequidar is being developed for oral administration as an intestine specific P-gp inhibitor, the potency of encequidar inhibition on P-gp in intestinal cells was also examined. To do this, the effect of encequidar on the intestinal permeability (efflux and absorption) of paclitaxel was evaluated in Caco-2 cells. The Caco-2 cell line is a human epithelial cell line derived from colorectal adenocarcinoma that expresses P-gp on the apical side and is widely used as a model of the intestinal epithelial barrier. In the absence of P-gp inhibitors, P-gp substrates, such as paclitaxel, are excluded from the basal ("absorption") experimental compartment into the apical compartment.

In our experiment, coadministration of encequidar with paclitaxel in the Caco-2 cell assay increased the apical to basal apparent permeability (P_{app} a → b, absorption) and decreased the basal to apical apparent permeability (P_{app} b → a, efflux) of paclitaxel. Based on these data, the IC_{50} of encequidar for inhibition of P-gp in Caco-2 intestinal cells was determined to be 53 nM, demonstrating that encequidar potently inhibits P-gp and prevents the efflux of paclitaxel from intestinal cells *in vitro*. This is consistent with the paclitaxel transcellular transport inhibition data in MDCK-MDR1 cells (an epithelial cell line of canine kidney origin and with high P-gp expression), where encequidar potently inhibited basal to apical transport of paclitaxel with an IC_{50} of ∼35 nM.[52]

Preclinical Pharmacokinetics (ADME). *Encequidar Alone.* Based on the excellent *in vitro* profile of encequidar, its preclinical pharmacokinetics were investigated (Table 4). To our delight, encequidar was minimally absorbed in both rats (C_{max} ∼10 nM) and dogs (C_{max} ∼39 nM) following oral dosing, and the bioavailability of encequidar after single oral doses was estimated to be 6.25% in rats and 11.2% in dogs. These results are in accordance with our observation in the Caco-2 permeability assay suggesting that encequidar has low absorption potential. The time to maximum plasma concentrations (T_{max}) was 8 h in rats and 13.3 h in dogs, indicating slow but prolonged absorption in the gastrointestinal tract with gradual excretion following oral dosing. Following daily repeat dosing (4 and 13 week) in rats and dogs, no significant systemic accumulation of plasma encequidar was observed, demonstrating that encequidar systemic exposure remains low even after repeated doses are administered. In the rat, encequidar appears to be absorbed at similarly low levels from all portions of the gastrointestinal tract, indicating that high exposure of encequidar in the gastrointestinal tract is achieved to allow for a complete P-gp inhibition, while systemic encequidar exposure is minimized to avoid systemic side effects.

Table 4. Plasma Pharmacokinetic Profile of Encequidar in Selected Preclinical Species

PK parameters	male Sprague-Dawley rat (n = 3)	male Beagle dog (n = 3)
dose IV/PO (mg/kg)	3/10	3/10
C_{max} (ng/mL)	7.1	26.6
T_{max} (h)	8.0	13.3
$T_{1/2}$ (h)	14.8	16.9
$AUC_{po,last}$ (ng·h/mL)	129.0	723.9
$AUC_{iv,last}$ (ng·h/mL)	618.8	1919.5
F (%)	6.25	11.2

Distribution studies in rats and dogs showed that the minimal concentrations of encequidar that are absorbed distribute to most tissues, except for the brain and spinal cord. However, the highest concentrations were observed in the liver and bile which is not surprising given that encequidar is excreted via the biliary route. *In vitro* studies show that encequidar is mainly metabolized by CYP3A4/5 and, to a lesser degree, by CYP1A2 and CYP2B6.

Encequidar with Oral Paclitaxel. Preclinical proof of concept pharmacokinetic studies with oral paclitaxel/encequidar were performed to evaluate if encequidar could inhibit P-gp in the GI tract to allow for the absorption of paclitaxel following oral dosing. In rats administered oral paclitaxel alone, low plasma concentrations and exposures of paclitaxel were achieved (C_{max} ∼127 ng/mL and AUC_{last} ∼308 ng·h/mL). In contrast, oral administration of paclitaxel in combination with encequidar as oral paclitaxel/encequidar increased both plasma concentrations and exposures of paclitaxel by approximately 10-fold. While in rats the oral bioavailability (F%) of paclitaxel was 41.3%, it ranged from 11 to 24% in dogs following oral dosing of paclitaxel/encequidar (Table 5, PK data in dogs not shown).[52] The bioavailability of paclitaxel achieved in both species demonstrates that encequidar facilitates the oral

Table 5. Oral Absorption of Paclitaxel Facilitated by Encequidar in Male Sprague-Dawley Rats[a]

PK parameters	paclitaxel alone (n = 4)	paclitaxel + encequidar (n = 9)
IV dose (mg/kg)	6	
PO dose (mg/kg)	20	20 + 10
CL (L/h)	2.1	
V_d (L)	23.6	
C_{max} PO (ng/mL)	127.2	1253.7
T_{max} (h)	PO 0.9, IV 0.08	PO 1.0
$T_{1/2}$ (h)	PO 8.0, IV 7.7	6.8
$AUC_{po,last}$ (ng·h/mL)	308.5	3756.5
$AUC_{iv,last}$ (ng·h/mL)	2728.1	
F (%)	3.4	41.3

[a]Adapted with permission from ref 52. Copyright 2010 Elsevier.

https://doi.org/10.1021/acs.jmedchem.0c01826
J. Med. Chem. 2021, 64, 3677−3693

Table 6. Response of Subcutaneous MDA-MB-231 Mammary Tumor to Treatment with Oral Paclitaxel/Encequidar or IV Paclitaxel[a]

group (admin route)	paclitaxel dose (mg/kg)	encequidar dose (mg/kg)	dosing schedule	tumor free survival/ total	days to two doublings	days delay (T/C)
saline control (PO)	0	0	Q2D×4	0/10	13.1	N/A
vehicle control (PO)[b]	0	0	Q2D×4	2/10	11.6	−1.5
paclitaxel (IV)	12	0	Q2D×4	1/10	26.1	13.0
	18	0	Q2D×4	5/10	>69.0[c]	>55.9[d]
oral paclitaxel/encequidar (PO)	20	8	Q2D×4	1/10	15.1	2.0
	30	12	Q2D×4	6/10	>69.0[c]	>55.9[d]
	40	16	Q2D×4	9/10	>69.0[c]	>55.9[d]

[a]IV, intravenous; N/A, not applicable; PO, oral gavage; Q2D×4, every other day for 4 doses; T/C, overall delay in growth of median tumor; n = 10/group. [b]The vehicle control is a combination of paclitaxel vehicle and encequidar vehicle (see the Supporting Information for details). [c]Only two animals in the IV paclitaxel group survived past day 69; as such, day 69 was determined as the cutoff. [d]Only one animal in the saline control group survived to day 61. As the delay calculation is dependent on the survival of the controls, 55.9 days was selected as the cutoff.

absorption of paclitaxel which results in appreciable systemic paclitaxel exposure *in vivo*.

Following oral paclitaxel/encequidar administration, paclitaxel demonstrated nonlinear plasma pharmacokinetics. Paclitaxel did not accumulate in rats or dogs when administered orally for 4 consecutive weeks as oral paclitaxel/encequidar. In both rats and dogs, the absorption of paclitaxel administered as oral paclitaxel/encequidar was inhibited by food. No significant gender differences were observed for paclitaxel following oral paclitaxel/encequidar administration in rats.

In mice and rats, paclitaxel distributed primarily to the liver, intestine, and kidney following administration of oral paclitaxel/encequidar. The paclitaxel tissue to plasma ratio in all organ tissues, excluding brain, was >1, indicating paclitaxel distribution to tissues is higher versus the plasma. The wide distribution of paclitaxel following oral paclitaxel/encequidar administration is similar to the distribution characteristics observed following IV administration of paclitaxel.[68] Based on the known human metabolism of paclitaxel after IV administration,[69] paclitaxel and its two metabolites (6α-hydroxypaclitaxel and 3′-*p*-hydroxypaclitaxel) were measured in dog plasma following a single oral paclitaxel/encequidar administration. The metabolite 6α-hydroxypaclitaxel had a metabolic ratio of 0.76, and 3′-*p*-hydroxypaclitaxel had a metabolic ratio of 0.01. Biliary excretion was the primary route of paclitaxel elimination in both rats and dogs. Both the metabolism and excretion of paclitaxel following oral paclitaxel/encequidar are in agreement with what has been described for IV paclitaxel.[68,69]

Assessment of the absorption, distribution, metabolism, and excretion (ADME) of paclitaxel following oral paclitaxel/encequidar data demonstrates that although encequidar alters the absorption of paclitaxel, it does not alter the distribution, metabolism, or excretion of paclitaxel. Thus, from a clinical safety perspective, the risks of oral paclitaxel/encequidar are expected to be consistent with other approved IV paclitaxel therapies.

In Vivo Efficacy of Oral Paclitaxel/Encequidar. As mentioned earlier, paclitaxel is a P-gp substrate whose clinical administration is limited to IV due to poor oral absorption caused by P-gp drug efflux in the small intestine. A previous study by Kwak et al. showed that oral coadministration of paclitaxel and encequidar effectively inhibited the tumor growth of human colon cancer cells (HT-29) in a xenograft model.[52] In that study, 40 mg/kg paclitaxel (in combination with 20 mg/kg encequidar) suppressed tumor growth by 94% and induced remission of tumor growth until day 47, an outcome superior to the IV paclitaxel arm included in the study. The results of this study demonstrate the ability of encequidar to inhibit P-gp and facilitate the absorption of paclitaxel to therapeutically effective plasma concentrations *in vivo*. Clinically, paclitaxel is used to treat many different types of cancers, including breast, lung, and ovarian cancer. Therefore, we examined additional tumor models to broaden the therapeutic potential of oral paclitaxel when given in combination with oral encequidar.

The first model we tested was a highly aggressive triple negative breast/mammary tumor cell (MDA-MB-231) mouse model. In female athymic NCr-nu mice (n = 10/group) implanted subcutaneously with MDA-MB-231 mammary tumor xenografts, oral paclitaxel was administered every other day for a total of four doses of 20, 30, or 40 mg/kg and encequidar was administered with paclitaxel at doses of 0 (PO vehicle control), 8, 12, or 16 mg/kg (paclitaxel:encequidar ratio 2.5:1). Intravenous (IV) paclitaxel was administered at doses of 12 or 18 mg/kg every other day for a total of four doses. Animals were monitored for 70 and 82 days after tumor implantation for changes in tumor weights and individual body weights, respectively. The median number of days for the tumors in each group to reach two tumor mass doublings were calculated with an evaluation period of 70 total days after the tumor was implanted. The median time to reach two tumor mass doublings was used in the calculation of the overall delay in the growth of the median tumor.

Body weight reduction was not noted at either dose level. Following oral paclitaxel/encequidar administration, median tumor growth delay was 2.0, >55.9, and >55.9 days, in the 20, 30, and 40 mg/kg (paclitaxel doses) oral paclitaxel/encequidar dose groups, respectively (Table 6). An average maximum weight loss of 5% was noted in both the 30 and 40 mg/kg oral paclitaxel/encequidar dose groups, respectively; however, no reduction was noted in the 20 mg/kg oral paclitaxel/encequidar dose group. Median tumor growth delay was −1.5 days in the vehicle control group. Compared to this control group, median tumor growth delay was 13.0 days in the 12 mg/kg IV paclitaxel dose group and >55.9 days in the 18 mg/kg IV paclitaxel dose group, suggesting the 12 mg/kg IV dosage does not provide adequate paclitaxel exposure, allowing residual disease to resume exponential growth. These findings demonstrate that 30 and 40 mg/kg oral paclitaxel/encequidar

https://doi.org/10.1021/acs.jmedchem.0c01826
J. Med. Chem. 2021, 64, 3677−3693

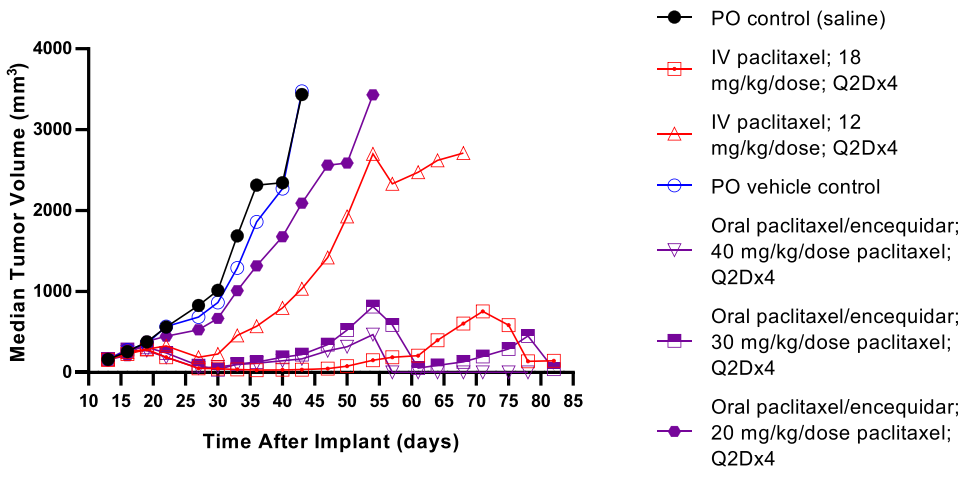

Figure 4. In vivo efficacy of oral paclitaxel/encequidar in mice bearing subcutaneous MDA-MB-231 mammary tumor xenografts (n = 10/group). Treatments were initiated on day 13.

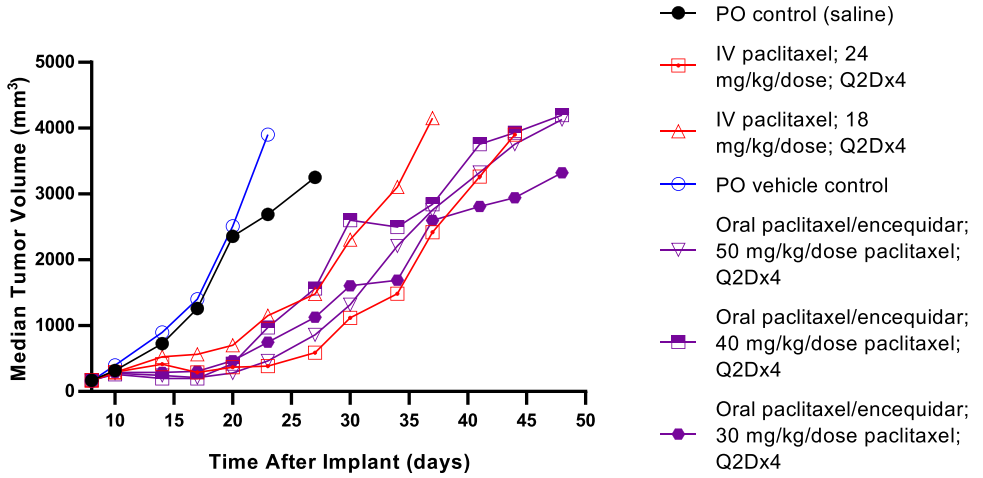

Figure 5. In vivo efficacy of oral paclitaxel/encequidar in mice bearing subcutaneous NCI-H460 human lung cancer xenografts (n = 10/group). Treatments were initiated on day 8.

reduced MDA-MB-231 tumor growth comparably to 18 mg/kg IV paclitaxel (Figure 4).

Another model tested was subcutaneously implanted NCI-H460 human lung tumor xenografts in mice. In this study, encequidar and oral paclitaxel were administered concomitantly as a single oral (gavage) solution to female athymic NCr-nu mice implanted subcutaneously with NCI-H460 tumor xenografts every other day for a total of four doses. Oral paclitaxel was administered at doses of 30, 40, or 50 mg/kg, and encequidar was administered with paclitaxel at doses of 12, 16, or 20 mg/kg (paclitaxel:encequidar ratio 2.5:1). For comparison, paclitaxel was also administered via IV on the same dosing schedule at doses of 18 and 24 mg/kg. The mice were monitored for 48 days post tumor implantation for changes in tumor weights and individual body weights.

There were no mortalities noted in the study, and body weight loss was similar among the IV and oral dosing groups. Median tumor growth delay was 8.5 and 16.3 days in the 18 and 24 mg/kg paclitaxel IV dose groups, respectively. Similarly, the median tumor growth delay was 9.9, 8.7, and 12.7 days in the 30, 40, and 50 mg/kg oral paclitaxel/encequidar dose groups, respectively. Following both routes of administration, tumor growth delay was the greatest following the highest dose of paclitaxel tested, demonstrating that when targeting NCI-H460 human lung tumors, oral paclitaxel/encequidar performed comparably to IV paclitaxel (Figure 5).

In addition to the breast and lung tumor models tested, other mouse tumor models that we have tested and which have shown that oral paclitaxel/encequidar is effective at inhibiting tumor growth include SK-OV-3 ovarian and vaginal epidermoid cancer cells (data not shown).

Preclinical Safety. To better understand encequidar and its potential for clinical use in combination with cytotoxic drugs, such as paclitaxel, for oral administration, the preclinical safety of encequidar alone and oral paclitaxel/encequidar combination was evaluated in rats (Sprague-Dawley) and dogs (Beagle).

Single oral administration of encequidar up to 2000 mg/kg/day to male and female Sprague–Dawley rats was well tolerated. No significant toxicity was noted following repeat encequidar administration in Sprague–Dawley rats or Beagle dogs. In rats administered encequidar for 4 and 13 weeks at doses up to 200 mg/kg/day, the only effects noted were in the mesenteric lymph nodes. Mesenteric lymph nodes were enlarged at doses $\geq$ 50 mg/kg, and histiocytosis in these lymph nodes was observed at doses $\geq$ 10 and 50 mg/kg, respectively. However, these findings were reversible and were considered an adaptive response to test article administration

https://doi.org/10.1021/acs.jmedchem.0c01826
J. Med. Chem. 2021, 64, 3677−3693

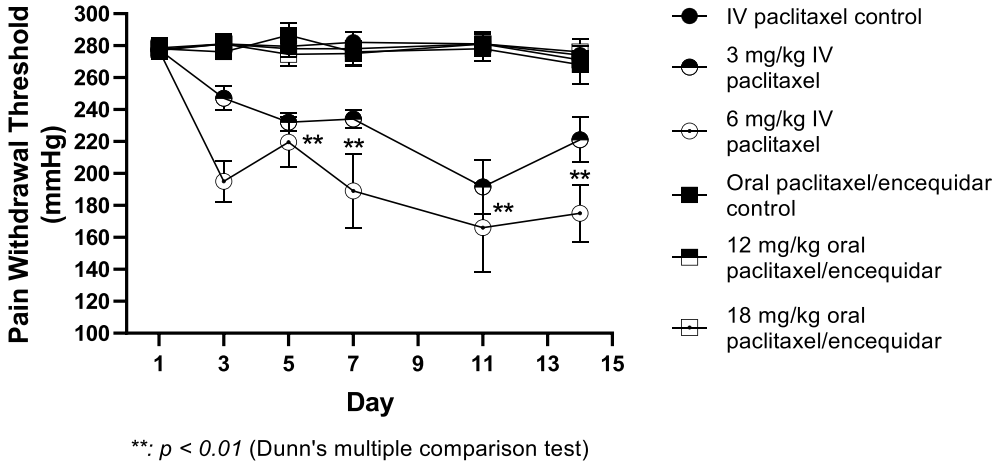

Figure 6. Measurement of nociceptive threshold in healthy rats treated with oral paclitaxel/encequidar and IV paclitaxel (Taxol). Statistical analysis was performed in GraphPad Prism version 5.0. If significance was recognized from the one-way analysis of variance results, Dunnett's test, a multiple comparison method, was performed to test the significant result of whether there is a difference between control group and administration group (n = 5/group).

and were not considered to be adverse in nature. Similarly, in Beagle dogs treated with encequidar for 13 weeks at encequidar doses up to 200 mg/day, an increase in total leukocyte (WBC) and eosinophil counts was noted at doses ≥ 100 mg/kg. Enlargement of mesenteric lymph nodes associated with microscopically observed histiocytosis was also observed at these doses. These findings were reversible and were considered of little toxicological significance because no other inflammatory reactions or functional effects were observed.

Repeat dose administration of oral paclitaxel/encequidar to rats and dogs resulted in toxicologically significant plasma exposure levels and caused toxicities characteristic of paclitaxel. The characteristic findings include leucopenia and anemia, bone marrow depression/atrophy, lymphoid atrophy, hepatic necrosis, and villous stunting and epithelial hyperplasia of the small intestine. Other target organs include the spleen and thymus. These toxicity findings are typical of those observed with paclitaxel after IV administration and were generally reversible or showed a tendency toward recovery following the 4−8 week recovery phases in the respective studies.

A major clinical dose limiting toxicity of paclitaxel is neuropathy, which correlates with high plasma concentrations of paclitaxel.[70] One of the advantages of oral paclitaxel/encequidar to patients is that the maximum plasma concentration (C_{max}) of paclitaxel achieved following administration is much lower than what is achieved following dosing of intravenous paclitaxel.[71] We postulated that the lower C_{max} of paclitaxel following oral paclitaxel/encequidar would result in less neuropathy compared to IV paclitaxel. To test this hypothesis, a rat safety study was performed which examined the neurotoxicity of paclitaxel following administration of oral paclitaxel/encequidar versus IV paclitaxel (Taxol). In this study, neurotoxicity was assessed by measuring the nociceptive threshold as indicated by pressure (mmHg) needed to produce a response, measured on the back paws of the healthy rats (Randall−Selitto test).[72] Oral paclitaxel was administered at doses of 12 and 18 mg/kg (cumulative dose 48 and 72 mg/kg). Encequidar was administered orally immediately prior to paclitaxel at doses of 6 and 9 mg/kg, respectively (paclitaxel/encequidar ratio was 2:1). Taxol was administered intravenously at doses of 0 (vehicle control), 3, 6 mg/kg (cumulative dose 12, 24 mg/kg) four times in 2-day intervals. Following dosing, the nociceptive threshold for the paw pressure test was statistically significantly reduced on days 5, 7, 11, and 14 following administration of 6 mg/kg IV paclitaxel versus its respective control group. In contrast, no significant reduction in the paw pressure test was noted following doses up to 18 mg/kg oral paclitaxel given in combination with 9 mg/kg encequidar, suggesting that oral paclitaxel/encequidar is less neurotoxic than IV paclitaxel in rats (Figure 6). Based on the encouraging overall preclinical data package that included favorable potency, target selectivity, pharmacokinetic, and safety profile, encequidar was advanced into clinical trials in humans.

Clinical Evaluation of Encequidar. The tolerability and pharmacokinetics of encequidar in humans was first reported by Kim et al. from a Phase 1, randomized, double-blind, placebo-controlled, single and multiple oral dosing, dose-escalation study in healthy male subjects.[73] Although absolute bioavailability was not defined, the results show that systemic exposure is low after oral administration at a single dose up to 900 mg (C_{max} = 6.6 ng/mL) or repeat dosing of five consecutive doses of up to 360 mg (C_{max} = 22.5 ng/mL). To evaluate the potential effects of encequidar on systemic P-gp activity and expression, lymphocytes and monocytes were isolated from subjects at the beginning and end of repeat dosing. Flow cytometry assays demonstrated that oral encequidar had minimal impact on *ex vivo* rhodamine 123 efflux and P-gp expression with a lack of dose−response across 60, 180, and 360 mg dose levels, indicating that oral encequidar has negligible systemic P-gp inhibition (unpublished results). In contrast, rhodamine 123 accumulation was enhanced in lymphocytes isolated from subjects post oral dosing of elacridar[74] and tariquidar,[75] systemically absorbed P-gp inhibitors. Exposure was also seen to increase with dose in a less than proportional manner, supporting that encequidar is poorly absorbed (unpublished results). The pharmacokinetics of encequidar can be described as having slow absorption and long elimination. Principal drug-related adverse events were diarrhea and abdominal pain, but all adverse events reported were mild in intensity and spontaneously resolved. The low grade and reversible adverse events associated with encequidar demonstrate its amenable safety profile for future combina-

https://doi.org/10.1021/acs.jmedchem.0c01826
J. Med. Chem. 2021, 64, 3677−3693

tions. Furthermore, the nature of toxicities that do occur support the localized action of encequidar in the gastrointestinal tract.

As a drug designed to induce a drug−drug interaction, multiple clinical interaction studies have been conducted to characterize the impact of encequidar on exposure and safety of clinically relevant substrates. These include two completed studies of the effect of encequidar on the oral pharmacokinetics of P-gp substrate loperamide[76,77] and ongoing interaction studies with oral P-gp substrates of narrow therapeutic index, digoxin and dabigatran etexilate, in healthy volunteers. Encequidar doses of 15 and 60 mg increased loperamide AUC_{last} by 1.46 and 1.63 times, respectively, and the effect of encequidar was maintained for 72 h after the administration but without affecting the CNS effects of loperamide. This is consistent with the designed localized effect of encequidar on the small intestine and low systemic concentrations in humans.

The pharmacokinetic aim of adding encequidar to an oral formulation of paclitaxel is for the combination to provide equivalent, if not superior, exposure above the minimum inhibitory concentration of systemic paclitaxel. The ability of encequidar to make paclitaxel, a highly insoluble and poorly absorbed P-gp substrate, bioavailable was demonstrated in a randomized crossover bioequivalence study with weekly intravenous paclitaxel in patients with advanced solid tumors.[71] Although IV paclitaxel was approved at a dosage of 175 mg/m^2 Q3W (every 3 weeks), the more widely used dosage of 80 mg/m^2 weekly was chosen as a clinically relevant comparator.[78] Based on population pharmacokinetic modeling, a dosing regimen of 15 mg oral encequidar given 1 h prior to 205 mg/m^2 oral paclitaxel three consecutive days per week was predicted to provide an equivalent total weekly exposure of IV paclitaxel. From 35 subjects evaluated for pharmacokinetics, oral paclitaxel yielded a weekly AUC (area under the curve) equivalent to 80 mg/m^2 IV paclitaxel with a 90% confidence interval of the geometric mean ratio within 80−125%. Critical to proving encequidar's effectiveness, the absolute bioavailability of oral paclitaxel was calculated as 11.8% at this bioequivalent dose level. The toxicity of oral paclitaxel/encequidar was primarily limited to diarrhea, vomiting, and fatigue. Consistent with the reduced neuropathy compared with IV paclitaxel, oral paclitaxel/encequidar produced an approximately seven times lower C_{max}.

Use of encequidar in combination with an oral formulation of paclitaxel has been explored in a variety of advanced malignancies where IV paclitaxel would previously be recommended or no approved therapies exist. For all indications tested, sequential oral administration of encequidar given 1 h prior to oral paclitaxel has achieved clinically efficacious paclitaxel levels. To assess the recommended Phase II dosages of oral paclitaxel/encequidar, Lee et al.[79] evaluated 24 patients with advanced cancers and identified that the effective plasma concentration of paclitaxel was achieved at a dose of 120 mg/m^2 following 60 mg/m^2 encequidar. Oral paclitaxel/encequidar was well tolerated. By obviating the use of IV paclitaxel excipient polyoxyl-35 castor oil,[80] oral paclitaxel/encequidar does not induce hypersensitivity. Therapeutic levels of paclitaxel (0.01 to 0.1 μM) were achieved without reaching the maximum tolerated dose; the only dose-limiting toxicity was a grade 3 neutropenia, observed at 240 mg/m^2 oral paclitaxel following 120 mg/m^2 oral encequidar.

The maximum tolerated dose of oral paclitaxel/encequidar was further explored in a Phase I/II with metastatic or recurrent gastric cancer. No dose limiting toxicity was reported, and oral paclitaxel and encequidar had a similar safety profile to IV paclitaxel, but with less peripheral neuropathy than conventional weekly paclitaxel.[81] Again, the maximum tolerated dose could not be determined for lack of toxicity, with neutropenia and diarrhea being the most common drug-related adverse events. At the recommended Phase II dose of 150 mg/m^2 oral paclitaxel with 15 mg oral encequidar (days 1, 2, 8, 9, 15, and 16 every 4 weeks), median progression-free survival and overall survival were 2.6 and 10.7 months, respectively, as a second-line therapy for patients with advanced gastric cancer.

A later, more dose-intense Phase I study of 34 patients with advance malignancies escalatedthe administration of oral paclitaxel/encequidar to a flat dose of 270 mg oral paclitaxel following 15 mg encequidar five consecutive days for 3 weeks of a 4 week cycle.[82] The most common treatment-related adverse events were nausea, diarrhea, anorexia, and vomiting. Serious treatment-related adverse events included febrile neutropenia, pneumonia, and dehydration. Again, the maximum tolerated dose was not reached, although two partial responses were observed in salivary gland and ovarian cancers at the 5 day dose level.

Evidence of the efficacy of oral paclitaxel/encequidar continues to be expanded with ongoing pivotal studies in angiosarcoma[83] (NCT03544567) and metastatic breast cancer[83] (NCT02594371). Oral paclitaxel/encequidar has showed encouraging efficacy and tolerability in the treatment of unresectable cutaneous angiosarcoma in an elderly population. Remarkably, all 26 patients showed reduction in tumor size, with 7 patients becoming eligible for curative resections after treatment.[84] In breast cancer, IV paclitaxel has been a backbone of chemotherapy treatment of advanced and metastatic disease but is associated with irreversible dose-limiting neuropathy and hypersensitivity in approximately half of all patients (Taxol monograph).[85] Oral paclitaxel/encequidar at a dosage of 15 mg encequidar given 1 h prior to 205 mg/m^2 oral paclitaxel three consecutive days per week (a dosage bioequivalent to IV) has recently demonstrated superior confirmed response, progression-free survival, and overall survival, with minimal clinically meaningful neuropathy in an ongoing open-label, randomized, multicenter, Phase III study against IV paclitaxel for metastatic breast cancer.[86] By replacing IV paclitaxel, these promising results open the potential for oral paclitaxel/encequidar to not only dramatically improve patient quality of life by enabling at-home care and reduction of irreversible neuropathy but also significantly improve efficacy over traditional chemotherapy. On the basis of extensive clinical studies, we have submitted a New Drug Application (NDA) to the FDA requesting the approval of oral paclitaxel/encequidar for metastatic breast cancer and the application has been granted priority review.[87]

CONCLUSIONS

In summary, by applying the fundamental principles of medicinal chemistry, we have developed the first-in-class intestine-specific P-gp inhibitor, encequidar (**14**), which has enabled the oral delivery of paclitaxel. The clinical pharmacokinetics of encequidar suggest minimal absorption with low systemic exposure at the dose of 15 mg broadly in line with the preclinical data. Oral paclitaxel/encequidar offers the possibility of improving the treatment outcome with no hypersensitivity and reduced neuropathy, while providing the

https://doi.org/10.1021/acs.jmedchem.0c01826
J. Med. Chem. 2021, 64, 3677−3693

convenience of at-home care for all cancers currently being treated with IV paclitaxel. The superior efficacy of oral paclitaxel/encequidar has already been demonstrated in a pivotal Phase III study of metastatic breast cancer. These promising clinical results encouraged us to file for the NDA submission. Future studies aim to broaden the utility of oral paclitaxel/encequidar to replace IV paclitaxel as a monotherapy and in a variety of established combination therapies for a diverse set of cancer types for which the prior generation of paclitaxel has established clinical impact.

EXPERIMENTAL SECTION

All reagents and chemicals were purchased from commercial suppliers and were used without further purification unless otherwise stated. ^{1}H NMR spectra were recorded at 400 MHz on a Bruker Avance III HD NMR spectrometer using DMSO-d_6 or $CDCl_3$ with TMS as the internal standard at ambient temperature. A Waters Alliance 2695 HPLC system equipped with a PDA detector (Waters 2998, 800 nm) was used. HPLC purity was determined by UV absorption at a wavelength of 254 nm (LC method: column XBridge C18, 5 μm, 150 × 4.6 mm at 25 ± 5 °C with a 0.8 mL/min flow rate; mobile phase A: 0.1% formic acid in water, mobile phase B: 0.1% formic acid in acetonitrile; 0.0−4.0 min, 90% A; 4.0−10.10, 95% B; 10.10−12.0 min, 90% A), and the mass ion was obtained by electrospray ionization. Chemical shifts are reported in parts per million (ppm, δ units). Coupling constants (J-values) are reported in units of hertz (Hz). Splitting patterns are abbreviated as s for singlet, d for doublet, t for triplet, q for quartet, m for multiplet, bs for broad singlet, and dd for doublet of doublet. The chemical yields reported are unoptimized. The purity of final test compounds was ≥95% as determined by ^{1}H NMR and HPLC. In all *in vitro*, animal, and clinical studies, encequidar was used in the methanesulfonate monohydrate form. The animal studies presented in this paper were reviewed and assessed by the Institutional Animal Care and Use Committee (IACUC). All animals used in the studies were cared for in accordance with the available guidelines for the care and use of laboratory animals (Association for Assessment and Accreditation of Laboratory Animal Care (AAALAC)).

4-(2-(6,7-Dimethoxy-3,4-dihydroisoquinolin-2(1*H*)-yl)-ethyl)aniline (22). To obtain **22**, 2.30 g (9.99 mmol) of 1-(2-bromoethyl)-4-nitrobenzene **19** and 2.29 g (9.97 mmol) of 6,7-dimethoxy-1,2,3,4-tetrahydroisoquinoline hydrochloride **20** were dissolved in 150 mL of DMF and then 4.15 g (30.0 mmol) of K_2CO_3 and 1.80 g (12.0 mmol) of NaI were added, and the mixture was allowed to react at 100 °C for 12 h. After mixing 150 mL of water, the reaction mixture was extracted three times with a 200 mL portion of EtOAc, and the combined organic layer was washed with saturated brine solution and dried over $MgSO_4$. The resulting solution was subjected to a reduced pressure to remove the solvent, and the residues was recrystallized using EtOAc to obtain 2.40 g of a nitro derivative **21** which was used in the next step without additional purification. Compound **21** was added to a mixture of THF and MeOH (1:1, 300 mL) and then 0.24 g of Pd/C was added, and the mixture was reduced under an atmospheric hydrogen pressure for 18 h. The resulting solution was filtered and concentrated under a reduced pressure to obtain 2.03 g (65% yield over 2 steps) of the title compound **22**. ^{1}H NMR (400 MHz, DMSO-d_6): δ 6.90 (d, J = 8.0 Hz, 2H), 6.65 (d, J = 8.4 Hz, 2H), 6.51 (d, J = 8.4 Hz, 2H), 4.81 (s, 2H), 3.70 (d, J = 2.0 Hz, 6H), 3.51 (s, 2H), 2.71−2.55 (m, 8H). Mass spec. m/z (ESI, +ve ion): 313.19 $(M + H)^+$.

(*E*)-*N*′(4,5-Dimethoxy-2-nitrobenzylidene)-4-methylbenzenesulfonohydrazide (25). To obtain **25**, 6.90 g (37.0 mmol) of *p*-toluenesulfonyl hydrazide **24** was dissolved in 40 mL of EtOH, and 7.90 g (37.4 mmol) of 6-nitroveratraldehyde **23** dissolved in a small amount of EtOH was added. The mixture was stirred at 80 °C for 30 min, cooled to room temperature, and mixed with 100 mL of water. The solid formed therein was filtered, washed with 100 mL of EtOH, and dried under reduced pressure to obtain 12.0 g (yield 85%) of the title compound **25**. ^{1}H NMR (400 MHz, DMSO-d_6): δ 11.73 (s, 1H), 8.35 (s, 1H), 7.81 (d, J = 8.4 Hz, 2H), 7.59 (s, 1H), 7.45 (d, J = 8.4 Hz, 2H), 7.15 (s, 1H), 3.89 (d, J = 3.6 Hz, 6H), 2.38 (s, 3H). Mass spec. m/z (ESI, +ve ion): 380.08 $(M + H)^+$.

2-(4-(5-(4,5-Dimethoxy-2-nitrophenyl)-2*H*-tetrazol-2-yl)-phenethyl)-6,7-dimethoxy-1,2,3,4-tetrahydroisoquinoline (26). To obtain **26**, 7.40 g (23.7 mmol) of compound **22** was added to 40 mL of 50% EtOH, and the mixture was cooled to 5 °C. Then 6.32 mL of 35% HCl and a solution obtained by dissolving 1.8 g (26.1 mmol) of sodium nitrite in 10 mL of water were added, and the mixture was cooled to −15 °C. An amount of 9 g (23.7 mmol) of compound **25** was dissolved in 140 mL of pyridine, by adding it slowly. The resulting solution was stirred for 14 h and washed with 1 N HCl. The organic layer was separated, dried over $MgSO_4$, filtered, and distilled under a reduced pressure. The residue was purified by silica gel column chromatography (0−5% MeOH/DCM) to obtain 9.0 g (yield 70%) of the title compound **26**. ^{1}H NMR (400 MHz, DMSO-d_6): δ 8.04 (d, J = 8.4 Hz, 2H), 7.76 (s, 1H), 7.59 (d, J = 8.0 Hz, 2H), 7.46 (s, 1H), 6.66 (d, J = 10.8 Hz, 2H), 3.96 (d, J = 3.2 Hz, 6H), 3.71 (s, 6H), 3.56 (s, 2H), 2.98−2.94 (m, 2H), 2.77−2.71 (m, 6H). Mass spec. m/z (ESI, +ve ion): 547.19 $(M + H)^+$.

2-(2-(4-(2-(6,7-Dimethoxy-3,4-dihydroisoquinolin-2(1*H*)-yl)-ethyl)phenyl)-2*H*-tetrazol-5-yl)-4,5-dimethoxyaniline (27). To obtain **27**, 0.25 g (0.46 mmol) of compound **26** was mixed with 3 mL of EtOH, 3 mL of DCM, and 0.07 g of Pd/C and stirred under a hydrogen atmosphere for 12 h at room temperature. The reaction mixture was filtered through a Celite pad, the pad was washed with EtOH, and the filtrate and wash solution were combined and distilled under a reduced pressure, to obtain 0.2 g (yield 85%) of the title compound **27**. ^{1}H NMR (400 MHz, $CDCl_3$): δ 8.11 (d, J = 8.4 Hz, 2H), 7.73 (s, 1H), 7.47 (d, J = 8.8 Hz, 2H), 6.63 (s, 1H), 6.56 (s, 1H), 6.37 (s, 1H), 5.33 (bs, 2H), 3.95 (s, 3H), 3.92 (s, 3H), 3.87 (d, J = 2.8 Hz, 6H), 3.69 (s, 2H), 3.04−3.01 (m, 2H), 2.88−2.83 (m, 6H). Mass spec. m/z (ESI, +ve ion): 517.18 $(M + H)^+$.

***N*-(2-(2-(4-(2-(6,7-Dimethoxy-3,4-dihydroisoquinolin-2(1*H*)-yl)ethyl)phenyl)-2*H*-tetrazol-5-yl)-4,5-dimethoxyphenyl)-quinoline-3-carboxamide (1).** To obtain **1**, 0.2 g (0.39 mmol) of **27** and 0.125 g (0.39 mmol) of thioester of quinoline-3-carboxylic acid (prepared by stirring a mixture of quinoline-3-carboxylic acid, triphenyl phosphine, 2,2′-benzothiazolyl disulfide, and Et_3N in DCM at room temperature overnight followed by filtering the obtained solid, washing with acetone, and drying under vacuum to obtain the desired thioester which was used without further purification) were added to 5 mL of DCM, and the mixture was stirred at room temperature for 12 h. After washing with 50 mL of distilled water, the organic layer was dried over $MgSO_4$, filtered, and distilled under a reduced pressure. The residue was subjected to silica gel column chromatography (0−5% MeOH/DCM) to obtain 0.18 g (yield 69%) of the title compound **1**. ^{1}H NMR (400 MHz, DMSO-d_6): δ 10.89 (s, 1H), 9.44 (d, J = 2.4 Hz, 1H), 9.01 (d, J = 2.0 Hz, 1H), 8.14 (d, J = 11.2 Hz, 1H), 8.05 (dd, J = 8.4 and 0.8 Hz, 1H), 7.96−7.90 (m, 4H), 7.74−7.70. (m, 2H), 7.44 (d, J = 8.8 Hz, 2H), 6.66 (d, J = 11.2 Hz, 2H), 3.90 (d, J = 1.6 Hz, 6H), 3.70 (d, J = 2.0 Hz, 6H), 3.55 (bs, 2H), 2.93 (t, J = 7.2 Hz, 2H), 2.71 (bs, 6H). Mass spec. m/z (ESI, +ve ion): 672.20 $(M + H)^+$. HPLC purity: 98.0%.

***N*-(2-(2-(4-(2-(6,7-Dimethoxy-3,4-dihydroisoquinolin-2(1*H*)-yl)ethyl)phenyl)-2*H*-tetrazol-5-yl)-4,5-dimethoxyphenyl)-quinoline-2-carboxamide (2).** To obtain **2**, 0.15 g (0.29 mmol) of **27** and 0.05 g (0.29 mmol) of quinaldic acid were added to 5 mL of DCM, and then 0.1 g (0.52 mmol) of EDCI·HCl and 0.005 g (0.041 mmol) of DMAP were added, and the mixture was stirred at room temperature for 12 h. After washing with 50 mL of distilled water, the organic layer was separated, dried over $MgSO_4$, filtered, and distilled under a reduced pressure. The residue was subjected to silica gel column chromatography (0−5% MeOH/DCM) to obtain 0.14 g (yield 73%) of the title compound **2**. ^{1}H NMR ($CDCl_3$): δ 12.60 (s, 1H), 8.71 (s, 1H), 8.40 (d, 2H), 8.20 (d, 2H), 8.13 (d, 1H), 7.90 (s, 2H), 7.65 (m, 2H), 7.37 (d, 2H), 6.58 (d, 2H), 4.05 (d, 6H), 3.85 (s, 6H), 3.67 (s, 2H), 3.01 (t, 2H), 2.83 (m, 6H).

***N*-(2-(2-(4-(2-(6,7-Dimethoxy-3,4-dihydroisoquinolin-2(1*H*)-yl)ethyl)phenyl)-2*H*-tetrazol-5-yl)-4,5-dimethoxyphenyl)-isoquinoline-3-carboxamide (3).** Following the procedure of

https://doi.org/10.1021/acs.jmedchem.0c01826
J. Med. Chem. 2021, 64, 3677−3693

compound **2** except 3-isoquinoline carboxylic acid was used instead of quinaldic acid, 0.12 g (yield 62%) of the title compound **3** was obtained. ^{1}H NMR ($CDCl_3$): δ 12.67 (s, 1H), 9.29 (s, 1H), 8.83 (s, 1H), 8.73 (s, 1H), 8.41 (d, 2H), 8.01 (d, 2H), 7.93 (s, 1H), 7.77 (m, 2H), 7.53 (d, 2H), 6.62 (s, 1H), 6.57 (s, 1H), 4.04 (d, 6H), 3.85 (s, 6H), 3.72 (s, 2H), 3.07 (t, 2H), 2.86 (m, 6H).

***N*-(2-(2-(4-(2-(6,7-Dimethoxy-3,4-dihydroisoquinolin-2(1*H*)-yl)ethyl)phenyl)-2*H*-tetrazol-5-yl)-4,5-dimethoxyphenyl)-quinoline-8-carboxamide (4).** Following the procedure of compound **2** except 8-quinoline carboxylic acid hydrate was used instead of quinaldic acid, 0.13 g (yield 67%) of the title compound **4** was obtained. ^{1}H NMR ($CDCl_3$): δ 13.69 (s, 1H), 8.87 (d, 1H), 8.77 (q, 1H), 8.37 (s, 1H), 8.24 (d, 1H), 8.06 (d, 1H), 8.00 (d, 2H), 7.38 (m, 1H), 7.23 (s, 1H), 6.58 (d, 2H), 4.03 (d, 6H), 3.85 (s, 6H), 3.65 (s, 2H), 2.95 (m, 2H), 2.81 (m, 6H).

***N*-(2-(2-(4-(2-(6,7-Dimethoxy-3,4-dihydroisoquinolin-2(1*H*)-yl)ethyl)phenyl)-2*H*-tetrazol-5-yl)-4,5-dimethoxyphenyl)-isoquinoline-1-carboxamide (5).** Following the procedure of compound **2** except 1-isoquinoline carboxylic acid was used instead of quinaldic acid, 0.12 g (yield 62%) of the title compound **5** was obtained. ^{1}H NMR ($CDCl_3$): δ 12.76 (s, 1H), 9.76 (d, 1H), 8.91 (s, 1H), 8.73 (d, 1H), 8.37 (d, 2H), 8.05 (s, 1H), 8.00 (m, 1H), 7.93 (d, 1H), 7.86 (m, 2H), 7.47 (d, 2H), 6.70 (d, 2H), 4.17 (d, 6H), 3.96 (s, 6H), 3.80 (s, 2H), 3.15 (t, 2H), 2.94 (m, 6H).

***N*-(2-(2-(4-(2-(6,7-Dimethoxy-3,4-dihydroisoquinolin-2(1*H*)-yl)ethyl)phenyl)-2*H*-tetrazol-5-yl)-4,5-dimethoxyphenyl)-isoquinoline-4-carboxamide (6).** Following the procedure of compound **2** except 4-isoquinoline carboxylic acid was used instead of quinaldic acid, 0.11 g (yield 57%) of the title compound **6** was obtained. ^{1}H NMR ($CDCl_3$): δ 11.38 (s, 1H), 9.09 (d, 1H), 8.74 (s, 1H), 8.52 (d, 1H), 8.23 (d, 1H), 7.89 (s, 1H), 7.79 (m, 4H), 7.64 (t, 1H), 7.36 (d, 2H), 6.62 (s, 1H), 6.55 (s, 1H), 4.08 (s, 3H), 4.01 (s, 3H), 3.85 (s, 6H), 3.67 (s, 2H), 2.98 (t, 2H), 2.82 (m, 6H).

***N*-(2-(2-(4-(2-(6,7-Dimethoxy-3,4-dihydroisoquinolin-2(1*H*)-yl)ethyl)phenyl)-2*H*-tetrazol-5-yl)-4,5-dimethoxyphenyl)-nicotinamide (7).** Following the procedure of compound **2** except 0.04 g of nicotinic acid was used instead of 0.05 g of quinaldic acid, 0.12 g (yield 67%) of the title compound **7** was obtained. ^{1}H NMR ($CDCl_3$) δ: 11.77 (s, 1H), 9.54 (s, 1H), 8.92 (d, 1H), 8.78 (s, 1H), 8.55 (d, 1H), 8.20 (d, 2H), 7.93 (s, 1H), 7.60 (m, 3H), 6.69 (d, 2H), 4.14 (d, 6H), 3.96 (d, 6H), 3.79 (s, 2H), 3.14 (t, 2H), 2.95 (m, 6H).

***N*-(2-(2-(4-(2-(6,7-Dimethoxy-3,4-dihydroisoquinolin-2(1*H*)-yl)ethyl)phenyl)-2*H*-tetrazol-5-yl)-4,5-dimethoxyphenyl)-2-naphthamide (8).** Following the procedure of compound **2** except 0.06 g of 2-naphthoic acid was used instead of 0.05 g of quinaldic acid, 0.15 g (yield 77%) of the title compound **8** was obtained. ^{1}H NMR ($CDCl_3$): δ 11.65 (s, 1H), 8.79 (s, 1H), 8.69 (s, 1H), 8.23 (d, 1H), 8.11 (d, 1H), 7.97 (m, 3H), 7.60 (m, 2H), 7.44 (m, 3H), 6.62 (s, 1H), 6.56 (s, 1H), 4.08 (s, 3H), 4.03 (s, 3H), 3.86 (s, 6H), 3.69 (s, 2H), 3.03 (t, 2H), 2.85 (m, 6H).

***N*-(2-(2-(4-(2-(6,7-Dimethoxy-3,4-dihydroisoquinolin-2(1*H*)-yl)ethyl)phenyl)-2*H*-tetrazol-5-yl)-4,5-dimethoxyphenyl)-pyrazine-2-carboxamide (9).** Following the procedure of compound **2** except 0.04 g of 2-pyrazine carboxylic acid was used instead of 0.05 g of quinaldic acid, 0.14 g (yield 78%) of the title compound **9** was obtained. ^{1}H NMR ($CDCl_3$): δ 12.47 (s, 1H), 9.56 (d, 1H), 8.83 (d, 1H), 8.73 (s, 1H), 8.70 (m, 1H), 8.30 (d, 2H), 7.93 (s, 1H), 7.52 (d, 2H), 6.59 (d, 2H), 4.05 (d, 6H), 3.86 (d, 6H), 3.86 (d, 6H), 3.70 (s, 2H), 3.06 (t, 2H), 2.85 (m, 6H).

***N*-(2-(2-(4-(2-(6,7-Dimethoxy-3,4-dihydroisoquinolin-2(1*H*)-yl)ethyl)phenyl)-2*H*-tetrazol-5-yl)-4,5-dimethoxyphenyl)-benzamide (10).** Following the procedure of compound **2** except benzoic acid was used instead of quinaldic acid, 0.15 g (yield 84%) of the title compound **10** was obtained. ^{1}H NMR ($CDCl_3$): δ 11.39 (s, 1H), 8.68 (s, 1H), 8.15 (d, 2H), 8.08 (d, 2H), 7.78 (s, 1H), 7.53 (m, 3H), 7.42 (d, 2H), 6.59 (s, 1H), 6.52 (s, 1H), 3.98 (d, 6H), 3.82 (s, 6H), 3.66 (s, 2H), 2.98 (t, 2H), 2.83 (m, 6H).

***N*-(2-(2-(4-(2-(6,7-Dimethoxy-3,4-dihydroisoquinolin-2(1*H*)-yl)ethyl)phenyl)-2*H*-tetrazol-5-yl)-4,5-dimethoxyphenyl)-3,4-difluorobenzamide (11).** Following the procedure of compound **2** except 0.06 g of 3,4-difluorobenzoic acid was used instead of 0.05 g of quinaldic acid, 0.12 g (yield 63%) of the title compound **11** was obtained. ^{1}H NMR ($CDCl_3$): δ 11.53 (s, 1H), 8.65 (s, 1H), 8.10 (d, 2H), 7.98 (m, 1H), 7.90 (m, 1H), 7.84 (s, 1H), 7.49 (d, 2H), 7.35 (d, 1H), 6.62 (s, 1H), 6.55 (s, 1H), 4.03 (d, 6H), 3.85 (s, 6H), 3.68 (s, 2H), 3.04 (t, 2H), 2.85 (m, 6H).

***N*-(2-(2-(4-(2-(6,7-Dimethoxy-3,4-dihydroisoquinolin-2(1*H*)-yl)ethyl)phenyl)-2*H*-tetrazol-5-yl)-4,5-dimethoxyphenyl)-thiophene-3-carboxamide (12).** Following the procedure of compound **2** except 3-thiophene carboxylic acid was used instead of quinaldic acid, 0.10 g (yield 55%) of the title compound **12** was obtained. ^{1}H NMR ($CDCl_3$): δ 11.43 (s, 1H), 8.63 (s, 1H), 8.21 (d, 1H), 8.08 (d, 2H), 7.76 (s, 1H), 7.74 (s, 1H), 7.48 (d, 2H), 7.38 (m, 1H), 6.61 (s, 1H), 6.54 (s, 1H), 3.99 (d, 6H), 3.83 (s, 6H), 3.67 (s, 2H), 3.02 (t, 2H), 2.83 (m, 6H).

***N*-(2-(2-(4-(2-(6,7-Dimethoxy-3,4-dihydroisoquinolin-2(1*H*)-yl)ethyl)phenyl)-2*H*-tetrazol-5-yl)-4,5-dimethoxyphenyl)-furan-3-carboxamide (13).** Following the procedure of compound **2** except 0.04 g of 3-furoic acid was used instead of 0.05 g of quinaldic acid, 0.05 g (yield 62%) of the title compound **13** was obtained. ^{1}H NMR ($CDCl_3$): δ 11.32 (s, 1H), 8.64 (s, 1H), 8.22 (s, 1H), 8.11 (d, 2H), 7.78 (s, 1H), 7.51 (m, 3H), 7.03 (d, 1H), 6.62 (s, 1H), 6.55 (s, 1H), 4.01 (d, 6H), 3.85 (s, 6H), 3.68 (s, 2H), 3.04 (t, 2H), 2.85 (m, 6H).

***N*-(2-(2-(4-(2-(6,7-Dimethoxy-3,4-dihydroisoquinolin-2(1*H*)-yl)ethyl)phenyl)-2*H*-tetrazol-5-yl)-4,5-dimethoxyphenyl)-4-oxo-4*H*-chromene-2-carboxamide (14).** To obtain **14**, 0.15 g (0.29 mmol) of **27** and 0.099 g of thioester of chromone-2-carboxylic acid (0.29 mmol) **28** (prepared by stirring a mixture of chromone-2-carboxylic acid, triphenyl phosphine, 2,2′-benzothiazolyl disulfide, and Et_3N in DCM at room temperature overnight followed by filtering the obtained solid, washing with acetone, and drying under vacuum to obtain the desired thioester which was used without further purification) were added to 5 mL of anhydrous DCM, and the mixture was stirred at room temperature for 12 h. After washing with 50 mL of distilled water, the organic layer was separated, dried over $MgSO_4$, filtered, and distilled under a reduced pressure. The residue was subjected to silica gel column chromatography (0−5% MeOH/DCM) to obtain 0.144 g (yield 72%) of the title compound **14**. ^{1}H NMR (400 MHz, DMSO-d_6): δ 11.72 (s, 1H), 8.06 (s, 1H), 7.99−7.96 (m, 1H), 7.91 (d, J = 8.0 Hz, 2H), 7.77−7.73 (m, 1H), 7.47−7.43 (m,5H), 6.80 (s, 1H), 6.67 (d, J = 8.4 Hz, 2H), 3.77 (d, J = 8.0 Hz, 6H), 3.71 (d, J = 1.6 Hz, 6H), 3.57 (s, 2H), 2.94 (t, J = 7.2 Hz, 2H), 2.75−2.72 (m, 6H). Mass spec. m/z (ESI, +ve ion): 689.31 (M + H)$^+$. HPLC purity: >99%.

***N*-(2-(2-(4-(2-(6,7-Dimethoxy-3,4-dihydroisoquinolin-2(1*H*)-yl)ethyl)phenyl)-2*H*-tetrazol-5-yl)-4,5-dimethoxyphenyl)-4-oxo-4*H*-chromene-3-carboxamide (15).** Following the procedure of compound **2** except 0.06 g of chromone-3-carboxylic acid was used instead of 0.05 g of quinaldic acid, 0.08 g (yield 40%) of the title compound **15** was obtained. ^{1}H NMR ($CDCl_3$): δ 12.15 (s, 1H), 9.04 (s, 1H), 8.89 (d, 1H), 8.50 (d, 2H), 7.60 (m, 3H), 7.49 (m, 3H), 7.04 (s, 1H), 6.55 (s, 1H), 6.54 (s, 1H), 4.04 (d, 6H), 3.84 (s, 6H), 3.67 (s, 2H), 3.03 (m, 2H), 2.84 (m, 6H).

***N*-(2-(2-(4-(2-(6,7-Dimethoxy-3,4-dihydroisoquinolin-2(1*H*)-yl)ethyl)phenyl)-2*H*-tetrazol-5-yl)-4,5-dimethoxyphenyl)-5-methoxy-4-oxo-4*H*-chromene-2-carboxamide (16).** Following the procedure of compound **2** except 0.3 g of **27** was used instead of 0.15 g of **27** and 0.19 g of 5-methoxychromone-2-carboxylic acid was used instead of 0.05 g of quinaldic acid, 0.23 g (yield 55%) of the title compound **16** was obtained. ^{1}H NMR ($CDCl_3$): δ 12.39 (s, 1H), 8.62 (d, 1H), 8.15 (d, 2H), 7.78 (s, 1H), 7.64 (t, 1H), 7.48 (d, 2H), 7.36 (d, 1H), 7.15 (s, 1H), 6.84 (d, 1H), 6.63 (s, 1H), 6.56 (s, 1H), 4.02 (m, 9H), 3.85 (s, 6H), 3.76 (s, 2H), 3.09 (m, 2H), 2.91 (m, 6H).

***N*-(2-(2-(4-(2-(6,7-Dimethoxy-3,4-dihydroisoquinolin-2(1*H*)-yl)ethyl)phenyl)-2*H*-tetrazol-5-yl)-4,5-dimethoxyphenyl)-6-fluoro-4-oxo-4*H*-chromene-2-carboxamide (17).** Following the procedure of compound **2** except 0.3 g of **27** was used instead of 0.15 g of **27** and 0.16 g of 6-fluorochromone-2-carboxylic acid was used instead of 0.05 g of quinaldic acid, 0.27 g (yield 66%) of the title compound **17** was obtained. ^{1}H NMR ($CDCl_3$): δ 12.60 (s, 1H), 8.66 (s, 1H), 8.17 (d, 2H), 7.92 (dd, 1H), 7.87 (dd, 1H), 7.82 (s, 1H),

https://doi.org/10.1021/acs.jmedchem.0c01826
J. Med. Chem. 2021, 64, 3677−3693

7.56 (m, 3H), 7.29 (s, 1H), 6.65 (s, 1H), 6.58 (s, 1H), 4.06 (d, 6H), 3.88 (s, 6H), 3.72 (s, 2H), 3.08 (m, 2H), 2.88 (m, 6H).

***N*-(2-(2-(4-(2-(6,7-Dimethoxy-3,4-dihydroisoquinolin-2(1*H*)-yl)ethyl)phenyl)-2*H*-tetrazol-5-yl)-4,5-dimethoxyphenyl)-6-methyl-4-oxo-4*H*-chromene-2-carboxamide (18).** Following the procedure of compound **2** except 0.08 g of 6-methylchromone-2-carboxylic acid was used instead of 0.05 g of quinaldic acid, 0.16 g (yield 79%) of the title compound **18** was obtained. ^{1}H NMR ($CDCl_3$): δ 12.49 (s, 1H), 8.62 (s, 1H), 8.14 (d, 2H), 8.02 (s, 1H), 7.78 (s, 1H), 7.69 (d, 1H), 7.57 (d, 1H), 7.47 (d, 2H), 6.58 (d, 2H), 4.02 (d, 6H), 3.85 (d, 6H), 3.68 (s, 2H), 3.04 (t, 2H), 2.82 (m, 6H), 2.49 (s, 3H).

■ ASSOCIATED CONTENT

Supporting Information

The Supporting Information is available free of charge at https://pubs.acs.org/doi/10.1021/acs.jmedchem.0c01826.

^{1}H NMR and HPLC chromatograms for **1** and **14**; experimental details for *in vitro* and *in vivo* studies (PDF)

Molecular formula strings and some data (CSV)

■ AUTHOR INFORMATION

Corresponding Author

Michael P. Smolinski − *Athenex Inc., Conventus Building, Buffalo, New York 14203, United States;* orcid.org/0000-0002-5303-2618; Email: msmolinski@athenex.com

Authors

Sameer Urgaonkar − *Athenex Inc., Conventus Building, Buffalo, New York 14203, United States;* orcid.org/0000-0002-6012-0923

Laura Pitzonka − *Athenex Inc., Conventus Building, Buffalo, New York 14203, United States*

Murray Cutler − *Athenex Inc., Conventus Building, Buffalo, New York 14203, United States*

GwanSun Lee − *Hanmi Pharmaceutical Co. Ltd., Songpa-gu, Seoul 05545, Korea*

Kwee Hyun Suh − *Hanmi Pharmaceutical Co. Ltd., Songpa-gu, Seoul 05545, Korea*

Johnson Y. N. Lau − *Athenex Inc., Conventus Building, Buffalo, New York 14203, United States*

Complete contact information is available at: https://pubs.acs.org/10.1021/acs.jmedchem.0c01826

Notes

The authors declare the following competing financial interest(s): M.P.S., S.U., L.P., M.C., and J.Y.N.L. are all employees of Athenex and hold equity in Athenex. G.L. and K.H.S. are employees of Hanmi.

■ ACKNOWLEDGMENTS

The authors are grateful to Professor Victor Ling and his team for discovering P-glycoprotein which form the basis for our work and thank Professor Ling personally for his encouragement. Additionally, we would like to acknowledge the years of effort and dedication from our Athenex and Hanmi colleagues who believed in this program and rallied behind the hope of bringing this important medication to patients. Special thanks are extended to David Hangauer, Ahmed Said, and Yahao Bu for significant contributions to preclinical understanding of Encequidar over the years.

■ DEDICATION

We gratefully honor the late Sung-Ki Lim, former Chairman of Hanmi Pharmaceuticals. Sung-Ki Lim's vision, dedication, and leadership were imperative to the development of this research program and his collaborative spirit was critical to the success of the partnership between Athenex Inc. and Hanmi Pharmaceuticals.

■ ABBREVIATIONS USED

P-gp, P-glycoprotein; BCRP, breast cancer resistance protein; MRP, multidrug resistance protein; BSEP, bile salt export pump; MATE, multidrug and toxin extrusion; OCT, organic cation transporter; OATP, organic anion transporting polypeptide; CYP, cytochrome P450; AUC, area under the curve; P_{app}, apparent permeability; IV, intravenous; CNS, central nervous system; tPSA, topological polar surface area; PK, pharmacokinetic; SAR, structure−activity relationship; EC_{50}, effective concentration giving 50% target inhibition; IC_{50}, inhibitory concentration giving 50% of maximal effect; MW, molecular weight; HBA, hydrogen bond acceptor; HBD, hydrogen bond donor; MDCK, Madin-Darby canine kidney cell; SC, subcutaneous; WBC, white blood cells; SILAC, stable isotope labeling with amino acids in cell culture; PO, per os (oral); ADME, absorption, distribution, metabolism, and excretion; ATPase, adenosine triphosphatase; Q3W, every 3 weeks; Q2D, every other day; QSAR, quantitative structure−activity relationship; NDA, New Drug Application; FDA, U.S. Food and Drug Administration; EMA, European Medicines Agency; WHO, World Health Organization; INN, International Nonproprietary Name.

■ REFERENCES

(1) Juliano, R. L.; Ling, V. A Surface Glycoprotein Modulating Drug Permeability in Chinese Hamster Ovary Cell Mutants. *Biochim. Biophys. Acta, Biomembr.* **1976**, *455*, 152−162.

(2) Gottesman, M. M.; Ling, V. The Molecular Basis of Multidrug Resistance in Cancer: The Early Years of P-glycoprotein Research. *FEBS Lett.* **2006**, *580*, 998−1009.

(3) Fojo, A. T.; Ueda, K.; Slamon, D. J.; Poplack, D. G.; Gottesman, M. M.; Pastan, I. Expression of a Multidrug-resistance Gene in Human Tumors and Tissues. *Proc. Natl. Acad. Sci. U. S. A.* **1987**, *84*, 265−269.

(4) Thiebaut, F.; Tsuruo, T.; Hamada, H.; Gottesman, M. M.; Pastan, I.; Willingham, M. C. Cellular Localization of the Multidrug-resistance Gene Product P-glycoprotein in Normal Human Tissues. *Proc. Natl. Acad. Sci. U. S. A.* **1987**, *84*, 7735−7738.

(5) Schinkel, A. H. P-glycoprotein, a Gatekeeper in the Blood-brain Barrier. *Adv. Drug Delivery Rev.* **1999**, *36*, 179−194.

(6) Eckford, P. D.; Sharom, F. J. ABC Efflux Pump-based Resistance to Chemotherapy Drugs. *Chem. Rev.* **2009**, *109*, 2989−3011.

(7) Szakács, G.; Paterson, J. K.; Ludwig, J. A.; Booth-Genthe, C.; Gottesman, M. M. Targeting Multidrug Resistance in Cancer. *Nat. Rev. Drug Discovery* **2006**, *5*, 219−234.

(8) Gottesman, M. M.; Fojo, T.; Bates, S. E. Multidrug Resistance in Cancer: Role of ATP-Dependent Transporters. *Nat. Rev. Cancer* **2002**, *2*, 48−58.

(9) List, A. F.; Kopecky, K. J.; Willman, C. L.; Head, D. R.; Persons, D. L.; Slovak, M. L.; Dorr, R.; Karanes, C.; Hynes, H. E.; Doroshow, J. H.; Shurafa, M.; Appelbaum, F. R. Benefit of Cyclosporine Modulation of Drug Resistance in Patients with Poor-risk Acute Myeloid Leukemia: a Southwest Oncology Group Study. *Blood* **2001**, *98*, 3212−3220.

(10) Eek, D.; Krohe, M.; Mazar, I.; Horsfield, A.; Pompilus, F.; Friebe, R.; Shields, A. L. Patient-reported Preferences for Oral Versus

Intravenous Administration for the Treatment of Cancer: a Review of the Literature. *Patient Preference and Adherence* **2016**, *10*, 1609−1621.
(11) Saloustros, E.; Mavroudis, D.; Georgoulias, V. Paclitaxel and Docetaxel in the Treatment of Breast Cancer. *Expert Opin. Pharmacother.* **2008**, *9*, 2603−2616.
(12) van Zuylen, L.; Verweij, J.; Sparreboom, A. Role of Formulation Vehicles in Taxane Pharmacology. *Invest. New Drugs* **2001**, *19*, 125−141.
(13) Vaclavikova, R.; Soucek, P.; Svobodova, L.; Anzenbacher, P.; Simek, P.; Guengerich, F. P.; Gut, I. Different In Vitro Metabolism of Paclitaxel and Docetaxel in Humans, Rats, Pigs, and Minipigs. *Drug Metab. Dispos.* **2004**, *32*, 666−674.
(14) Leu, B.-L.; Lai, M.-D.; Huang, J-d. Induction and Inhibition of Intestinal P-glycoprotein and Effects on Etoposide Absorption. *Yakubutsu Dotai* **1993**, *8*, 727−730.
(15) (a) Tsuruo, T.; Iida, H.; Tsukagoshi, S.; Sakurai, Y. Overcoming of Vincristine Resistance in P388 Leukemia *in Vivo* and *in Vitro* through Enhanced Cytotoxicity of Vincristine and Vinblastine by Verapamil. *Cancer Res.* **1981**, *41*, 1967−1972. (b) Twentyman, P. R.; Fox, N. E.; White, D. J. G. Cyclosporin A and its Analogues as Modifiers of Adriamycin and Vincristine Resistance in a Multi-drug Resistant Human Lung Cancer Cell Line. *Br. J. Cancer* **1987**, *56*, 55−57.
(16) Terwogt, J. M. M.; Malingré, M. M.; Beijnen, J. H.; ten Bokkel Huinink, W. W.; Rosing, H.; Koopman, F. J.; van Tellingen, O.; Swart, M.; Schellens, J. H. M. Coadministration of Oral Cyclosporin A Enables Oral Therapy with Paclitaxel. *Clin. Cancer Res.* **1999**, *5*, 3379−3384.
(17) Terwogt, J. M. M.; Beijnen, J. H.; ten Bokkel Huinink, W. W.; Rosing, H.; Schellens, J. H. Co-administration of Cyclosporin Enables Oral Therapy with Paclitaxel. *Lancet* **1998**, *352*, 285.
(18) Kröger, N.; Lehnert, M.; Mross, K.; Gieseking, F.; Thürlimann, B.; Schüller, F.; Kupper, H.; Hossfeld, D. K. Dexverapmil to Overcome Anthracycline-Resistant in Advanced Breast Cancer. *Eur. J. Cancer* **1995**, *31*, S79.
(19) Gaveriaux, C.; Boesch, D.; Jachez, B.; Bollinger, P.; Payne, T.; Loor, F. SDZ PSC 833, a Non-immunosuppressive Cyclosporin Analog, is a Very Potent Multidrug-Resistance Modifier. *J. Cell Pharmacol.* **1991**, *2*, 225−234.
(20) Boesch, D.; Gavériaux, C.; Jachez, B.; Pourtier-Manzanedo, A.; Bollinger, P.; Loor, F. *In Vivo* Circumvention of P-glycoprotein-Mediated Multidrug Resistance of Tumor Cells with SDZ PSC 833. *Cancer Res.* **1991**, *51*, 4226−4233.
(21) Kang, M. H.; Figg, W. D.; Ando, Y.; Blagosklonny, M. V.; Liewehr, D.; Fojo, T.; Bates, S. E. The P-Glycoprotein Antagonist PSC 833 Increases the Plasma Concentrations of 6α-Hydroxypaclitaxel, a Major Metabolite of Paclitaxel. *Clin. Cancer Res.* **2001**, *7*, 1610−1617.
(22) Greenberg, P. L.; Lee, S. J.; Advani, R.; Tallman, M. S.; Sikic, B. I.; Letendre, L.; Dugan, K.; Lum, B.; Chin, D. L.; Dewald, G.; Paietta, E.; Bennett, J. M.; Rowe, J. M. Mitoxantrone, Etoposide, and Cytarabine With or Without Valspodar in Patients With Relapsed or Refractory Acute Myeloid Leukemia and High-Risk Myelodysplastic Syndrome: A Phase III Trial (E2995). *J. Clin. Oncol.* **2004**, *22*, 1078−1086.
(23) Traunecker, H. C. L.; Stevens, M. C. G.; Kerr, D. J.; Ferry, D. R. The acridonecarboxamide GF120918 Potently Reverses P-glycoprotein-mediated Resistance in Human Sarcoma MES-Dx5 Cells. *Br. J. Cancer* **1999**, *81*, 942−951.
(24) Malingré, M. M.; Beijnen, J. H.; Rosing, H.; Koopman, F. J.; Jewell, R. C.; Paul, E. M.; Ten Bokkel Huinink, W. W.; Schellens, J. H. M. Co-administration of GF120918 Significantly Increases the Systemic Exposure to Oral Paclitaxel in Cancer Patients. *Br. J. Cancer* **2001**, *84*, 42−47.
(25) Fox, E.; Bates, S. E. Tariquidar (XR9576): Drug Efflux Pump Inhibitor. *Expert Rev. Anticancer Ther.* **2007**, *7*, 447−459.
(26) Newman, M. J.; Rodarte, J. C.; Benbatoul, K. D.; Romano, S. J.; Zhang, C.; Krane, S.; Moran, E. J.; Uyeda, R. T.; Dixon, R.; Guns, E. S.; Mayer, L. D. Discovery and Characterization of OC144−093, a Novel Inhibitor of P-Glycoprotein-mediated Multidrug Resistance. *Cancer Res.* **2000**, *60*, 2964−2972.
(27) Kuppens, I. E. L. M.; Bosch, T. M.; van Maanen, M. J.; Rosing, H.; Fitzpatrick, A.; Beijnen, J. H.; Schellens, J. H. M. Oral Bioavailability of Docetaxel in Combination with OC144−093 (ONT-093). *Cancer Chemother. Pharmacol.* **2005**, *55*, 72−78.
(28) Dantzig, A. H.; Shepard, R. L.; Cao, J.; Law, K. L.; Ehlhardt, W. J.; Baughman, T. M.; Bumol, T. F.; Starling, J. J. Reversal of P-glycoprotein-mediated Multidrug Resistance by a Potent Cyclopropyldibenzosuberane Modulator, LY335979. *Cancer Res.* **1996**, *56*, 4171−4179.
(29) Sandler, A.; Gordon, M.; de Alwis, D. P.; Pouliquen, I.; Green, L.; Marder, P.; Chaudhary, A.; Fife, K.; Battiato, L.; Sweeney, C.; Jordan, C.; Burgess, M.; Slapak, C. A. A Phase I Trial of a Potent P-Glycoprotein Inhibitor, Zosuquidar Trihydrochloride (LY335979), Administered Intravenously in Combination with Doxorubicin in Patients with Advanced Malignancy. *Clin. Cancer Res.* **2004**, *10*, 3265−3272.
(30) van Zuylen, L.; Sparreboom, A.; van der Gaast, A.; Nooter, K.; Eskens, F. A. L. M.; Brouwer, E.; Bol, C. J.; de Vries, R.; Palmer, P. A.; Verweij, J. Disposition of Docetaxel in the Presence of P-glycoprotein Inhibition by Intravenous Administration of R101933. *Eur. J. Cancer* **2002**, *38*, 1090−1099.
(31) van Zuylen, L.; Sparreboom, A.; van der Gaast, A.; van der Burg, M. E. L.; van Beurden, V.; Bol, C. J.; Woestenborghs, R.; Plamer, P. A.; Verweij, J. The Orally Administered P-glycoprotein Inhibitor R101933 Does Not Alter the Plasma Pharmacokinetics of Docetaxel. *Clin. Cancer Res.* **2000**, *6*, 1365−1371.
(32) Koolen, S. L. W.; Beijnen, J. H.; Schellens, J. H. M. Intravenous-to-Oral Switch in Anticancer Chemotherapy: A Focus on Docetaxel and Paclitaxel. *Clin. Pharmacol. Ther.* **2010**, *87*, 126−129.
(33) Lipinski, C. A.; Lombardo, F.; Dominy, B. W.; Feeney, P. J. Experimental and Computational Approaches to Estimate Solubility and Permeability in Drug Discovery and Development Settings. *Adv. Drug Delivery Rev.* **1997**, *23*, 3−25.
(34) Al-Shawi, M. K.; Omote, H. The Remarkable Transport Mechanism of P-glycoprotein; a Multidrug Transporter. *J. Bioenerg. Biomembr.* **2005**, *37*, 489−496.
(35) Frank, G. A.; Shukla, S.; Rao, P.; Borgnia, M. J.; Bartesaghi, A.; Merk, A.; Mobin, A.; Esser, L.; Earl, L. A.; Gottesman, M. M.; Xia, D.; Ambudkar, S. V.; Subramaniam, S. Cryo-EM Analysis of the Conformational Landscape of Human P-glycoprotein (ABCB1) During its Catalytic Cycle. *Mol. Pharmacol.* **2016**, *90*, 35−41.
(36) Sharom, F. J. Complex Interplay Between the P-glycoprotein Multidrug Efflux Pump and the Membrane: Its Role in Modulating Protein Function. *Front. Oncol.* **2014**, *4*, 41.
(37) Xia, D.; Zhou, F.; Esser, L. Emerging Consensus on the Mechanism of Polyspecific Substrate Recognition by the Multidrug Transporter P-glycoprotein. *Cancer Drug Resist.* **2019**, *2*, 471−489.
(38) Arana, M. R.; Altenberg, G. A. ATP-binding Cassette Exporters: Structure and Mechanism with a Focus on P-glycoprotein and MRP1. *Curr. Med. Chem.* **2019**, *26*, 1062−1078.
(39) Roe, M.; Folkes, A.; Ashworth, P.; Brumwell, J.; Chima, L.; Hunjan, S.; Pretswell, I.; Dangerfield, W.; Ryder, H.; Charlton, P. Reversal of P-glycoprotein Mediated Multidrug Resistance by Novel Anthranilamide Derivatives. *Bioorg. Med. Chem. Lett.* **1999**, *9*, 595−600.
(40) Ryder, H.; Ashworth, P. A.; Roe, M. J.; Brumwell, J.; Hunjan, S.; Folkes, A.; Sanderson, J. Anthranilic Acid Derivatives as Multi Drug Resistance Modulators. WO98/17648, April 30, 1998.
(41) Pajeva, I. K.; Wiese, M. Structural-Activity Relationships of Tariquidar Analogs as Multidrug Resistance Modulators. *AAPS J.* **2009**, *11*, 435−444.
(42) (a) Kreisl, W. C.; Bhatia, R.; Morse, C. L.; Woock, A. E.; Zoghbi, S. S.; Shetty, H. U.; Pike, V. W.; Innis, R. B. Increased Permeability-Glycoprotein Inhibition at the Human Blood-Brain Barrier Can Be Safely Achieved by Performing PET During Peak Plasma Concentrations of Tariquidar. *J. Nucl. Med.* **2015**, *56*, 82−87.

https://doi.org/10.1021/acs.jmedchem.0c01826
J. Med. Chem. 2021, 64, 3677−3693

(b) Matzneller, P.; Kussmann, M.; Eberl, S.; Maier-Salamon, A.; Jäger, W.; Bauer, M.; Langer, O.; Zeitlinger, M.; Poeppl, W. Pharmacokinetics of the P-gp Inhibitor Tariquidar in Rats After Intravenous, Oral, and Intraperitoneal Administration. *Eur. J. Drug Metab. Pharmacokinet.* **2018**, *43*, 599−606.
(43) Veber, D. F.; Johnson, S. R.; Cheng, H.-Y.; Smith, B. R.; Ward, K. W.; Kopple, K. D. Molecular Properties That Influence the Oral Bioavailability of Drug Candidates. *J. Med. Chem.* **2002**, *45*, 2615−2623.
(44) Kelder, J.; Grootenhuis, P. D. J.; Bayada, D. M.; Delbressine, L. P. C.; Ploemen, J.-P. Polar Molecular Surface as a Dominating Determinant for Oral Absorption and Brain Penetration of Drugs. *Pharm. Res.* **1999**, *16*, 1514−1519.
(45) (a) Palm, K.; Stenberg, P.; Luthman, K.; Artursson, P. Polar Molecular Surface Properties Predict the Intestinal Absorption of Drugs in Humans. *Pharm. Res.* **1997**, *14*, 568−571. (b) Lu, J. J.; Crimin, K.; Goodwin, J. T.; Crivori, P.; Orrenius, C.; Xing, L.; Tandler, P. J.; Vidmar, T. J.; Amore, B. M.; Wilson, A. G. E.; Stouten, P. F. W.; Burton, P. S. J. Influence of Molecular Flexibility and Polar Surface Area Metrics on Oral Bioavailability in the Rat. *J. Med. Chem.* **2004**, *47*, 6104−6107.
(46) Planting, A. S. T.; Sonneveld, P.; van der Gaast, A.; Sparreboom, A.; van der Burg, M. E. L.; Luyten, G. P. M.; de Leeuw, K.; de Boer-Dennert, M.; Wissel, P. S.; Jewell, R. C.; Paul, E. M.; Purvis, N. B., Jr.; Verweij, J. A Phase I and Pharmacologic Study of the MDR Converter GF120918 in Combination with Doxorubicin in Patients with Advanced Solid Tumors. *Cancer Chemother. Pharmacol.* **2005**, *55*, 91−99.
(47) Ertl, P.; Rohde, B.; Selzer, P. Fast Calculation of Molecular Polar Surface Area as a Sum of Fragment-Based Contributions and Its Application to the Prediction of Drug Transport Properties. *J. Med. Chem.* **2000**, *43*, 3714−3717.
(48) Zabrocki, J.; Smith, G. D.; Dunbar, J. B., Jr.; Iijima, H.; Marshall, G. R. Conformational Mimicry: 1. 1,5-Disubstituted Tetrazole Ring as a Surrogate for the Cis-Amide Bond. *J. Am. Chem. Soc.* **1998**, *110*, 5875−5880.
(49) Neochoritis, C. G.; Zhao, T.; Dömling, A. Tetrazoles via Multicomponent Reactions. *Chem. Rev.* **2019**, *119*, 1970−2042.
(50) Kaminsky, L. S.; Zhang, Q.-Y. The Small Intestine as a Xenobiotic-Metabolizing Organ. *Drug Metab. Dispos.* **2003**, *31*, 1520−1525.
(51) Bang, K. C.; Cha, M. Y.; Ahn, Y. G.; Ham, Y. J.; Kim, M. S.; Lee, G. S. P-glycoprotein Inhibitor, Method for Preparing the Same and Pharmaceutical Composition Comprising the Same. U.S. Patent 7,625,926 B2, December 1, 2009.
(52) Kwak, J.-O.; Lee, S. H.; Lee, G. S.; Kim, M. S.; Ahn, Y.-G.; Lee, J. H.; Kim, S. W.; Kim, K. H.; Lee, M. G. Selective Inhibition of MDR1 (ABCB1) by HM30181 Increases Oral Bioavailability and Therapeutic Efficacy of Paclitaxel. *Eur. J. Pharmacol.* **2010**, *627*, 92−98.
(53) Ito, S.; Tanaka, Y.; Kakehi, A.; Kondo, K. A Facile Synthesis of 2,5-Disubstituted Tetrazoles by the Reaction of Phenylsulfonylhydrazones with Arenediazonium Salts. *Bull. Chem. Soc. Jpn.* **1976**, *49*, 1920−1923.
(54) Topological polar surface area and log *P* were calculated using Molinspiration Property Calculation Service. https://www.molinspiration.com/cgi-bin/properties (accessed 2020-10-15).
(55) Bindu, R.; Srinivas, P.; Ravindrababu, D. S. Formulation and Characterization of Parenteral In Situ Implants of Tariquidar Bimesylate. *Int. J. Pharm. Sci. Res.* **2015**, *6*, 2028−2034.
(56) Sane, R.; Mittapalli, R. K.; Elmquist, W. F. Development and Evaluation of a Novel Microemulsion Formulation of Elacridar to Improve its Bioavailability. *J. Pharm. Res.* **2013**, *102*, 1343−1354.
(57) Ma, N.; Zhang, Z.-M.; Lee, J.-S.; Cheng, K.; Lin, L.; Zhang, D.-M.; Hao, P.; Ding, K.; Ye, W.-C.; Li, Z. Affinity-Based Protein Profiling Reveals Cellular Targets of Photoreactive Anticancer Inhibitors. *ACS Chem. Biol.* **2019**, *14*, 2546−2552.
(58) Sprachman, M. M.; Laughney, A. M.; Kohler, R. H.; Weissleder, R. In Vivo Imaging of Multidrug Resistance Using a Third Generation MDR1 Inhibitor. *Bioconjugate Chem.* **2014**, *25*, 1137−1142.
(59) Alam, A.; Kowal, J.; Broude, E.; Roninson, I.; Locher, K. P. Structural Insight into Substrate and Inhibitor Discrimination by Human P-glycoprotein. *Science* **2019**, *363*, 753−756.
(60) Alam, A.; Küng, R.; Kowal, J.; mcLeod, R. A.; Tremp, N.; Broude, E. V.; Roninson, I. B.; Stahlberg, H.; Locher, K. P. Structural of a Zosuquidar and UIC2-Bound Human-Mouse Chimeric ABCB1. *Proc. Natl. Acad. Sci. U. S. A.* **2018**, *115*, E1973−E1982.
(61) Kim, Y.; Chen, J. Molecular Structure of Human P-glycoprotein in the ATP-Bound, Outward-Facing Conformation. *Science* **2018**, *359*, 915−919.
(62) Lusvarghi, S.; Robey, R. W.; Gottesman, M. M.; Ambudkar, S. V. Multidrug Transporters: Recent Insights from Cryo-Electron Microscopy-Derived Atomic Structures and Animal Models. *F1000Research* **2020**, *9*, 9.
(63) (a) Aller, S. G.; Yu, J.; Ward, A.; Weng, Y.; Chittaboina, S.; Zhuo, R.; Harrell, P. M.; Trinh, Y. T.; Zhang, Q.; Urbatsch, I. L.; Chang, G. Structure of P-glycoprotein Reveals a Molecular Basis for Poly-specific Drug Binding. *Science* **2009**, *323*, 1718−1722. (b) Li, J.; Jaimes, K. F.; Aller, S. G. Refined Structures of Mouse P-glycoprotein. *Protein Sci.* **2014**, *23*, 34−46.
(64) Trott, O.; Olson, A. J. AutoDock Vina: Improving the Speed and Accuracy of Docking with a New Scoring Function, Efficient Optimization, and Multithreading. *J. Comput. Chem.* **2010**, *31*, 455−461.
(65) McCormick, J. W.; Vogel, P. D.; Wise, J. G. Multiple Drug Transport Pathways through Human P-glycoprotein. *Biochemistry* **2015**, *54*, 4374−4390.
(66) Ferreira, R. J.; Ferreira, M-J. U.; dos Santos, D. J. V. A. Molecular Docking Characterizes Substrate-Binding Sites and Efflux Modulation Mechanisms within P-glycoprotein. *J. Chem. Inf. Model.* **2013**, *53*, 1747−1760.
(67) (a) Loo, T. W.; Clarke, D. M. Mapping the Binding Site of the Inhibitor Tariquidar Stabilizes the First Transmembrane Domain of P-glycoprotein. *J. Biol. Chem.* **2015**, *290*, 29389−29401. (b) Labrie, P.; Maddaford, S. P.; Fortin, S.; Rakhit, S.; Kotra, L. P.; Gaudreault, R. C. A Comparative Molecular Field Analysis (CoMFA) and Comparative Molecular Similarity Indices Analysis (CoMSIA) of Anthranilamide Derivatives That Are Multidrug Resistance Modulators. *J. Med. Chem.* **2006**, *49*, 7646−7660.
(68) Sparreboom, A.; van Tellingen, O.; Nooijen, W. J.; Beijnen, J. H. Tissue Distribution, Metabolism and Excretion of Paclitaxel in Mice. *Anti-Cancer Drugs* **1996**, *7*, 78−86.
(69) Gianni, L.; Kearns, C. M.; Giani, A.; Capri, G.; Viganó, L.; Lacatelli, A.; Bonadonna, G.; Egorin, M. J. Nonlinear Pharmacokinetics and Metabolism of Paclitaxel and its Pharmacokinetic/Pharmacodynamic Relationships in Humans. *J. Clin. Oncol.* **1995**, *13*, 180−190.
(70) Postma, T. J.; Vermorken, J. B.; Liefting, A. J.; Pinedo, H. M.; Heimans, J. J. Paclitaxel-induced Neuropathy. *Ann. Oncol.* **1995**, *6*, 489−94.
(71) Jackson, C. G. C. A.; Deva, S.; Bayston, K.; McLaren, B.; Barlow, P.; Hung, N. A.; Clarke, K.; Segelov, E.; Chao, T.; Dai, M.; Yen, H.; Ang, E.; Cutler, D.; Kramer, D.; Zhi, J.; Chan, W.; Kwan, M. R.; Hung, C. An International Randomized Cross-over Bioequivalence Study of Oral Paclitaxel + HM30181 Compared with Weekly Intravenous (IV) Paclitaxel in Patients with Advanced Solid Tumours. *Ann. Oncol.* **2019**, *30*, 180−181.
(72) Randall, L. O.; Selitto, J. J. A Method for Measurement of Analgesic Activity on Inflammed Tissue. *Arch. Int. Pharmacodyn. Ther.* **1957**, *111*, 409−419.
(73) Kim, T.-E.; Gu, N.; Yoon, S. H.; Cho, J.-Y.; Park, K.-M.; Shin, S.-G.; Jang, I.-J.; Yu, K.-S. Tolerability and Pharmacokinetics of a New P-glycoprotein Inhibitor, HM30181, in Healthy Korean Male Volunteers: Single- and Multiple-dose Randomized, Placebo-controlled Studies. *Clin. Ther.* **2012**, *34*, 482−494.

https://doi.org/10.1021/acs.jmedchem.0c01826
J. Med. Chem. 2021, 64, 3677−3693

(74) Witherspoon, S. M.; Emerson, D. L.; Kerr, B. M.; Lloyd, T. L.; Dalton, W. S.; Wissel, P. S. Flow Cytometric Assay of Modulation of P-glycoprotein Function in Whole Blood by the Multidrug Resistance Inhibitor GG918. *Clin. Cancer Res.* **1996**, *2*, 7−12.
(75) Stewart, A.; Steiner, J.; Mellows, G.; Laguda, B.; Norris, D.; Bevan, P. Phase I Trial of XR9576 in Healthy Volunteers Demonstrates Modulation of P-glycoprotein in CD56+ Lymphocytes After Oral and Intravenous Administration. *Clin. Cancer Res.* **2000**, *6*, 4186−4191.
(76) Cha, Y.-J.; Lee, H.; Gu, N.; Kim, T.-E.; Lim, K. S.; Yoon, S. H.; Chung, J.-Y.; Jang, I.-J.; Shin, S.-G.; Yu, K.-S.; Cho, J.-Y. Sustained Increase in the Oral Bioavailability of Loperamide After a Single Oral Dose of HM30181, a P-glycoprotein Inhibitor, in Healthy Male Participants. *Basic Clin. Pharmacol. Toxicol.* **2013**, *113*, 419−424.
(77) Kim, T.-E.; Lee, H.; Lim, K. S.; Lee, S.; Yoon, S.-H.; Park, K.-M.; Han, H.; Shin, S.-G.; Jang, I.-J.; Yu, K.-S.; Cho, J.-Y. Effects of HM30181, a P-glycoprotein Inhibitor, on the Pharmacokinetics and Pharmacodynamics of Loperamide in Healthy Volunteers. *Br. J. Clin. Pharmacol.* **2014**, *78*, 556−564.
(78) Sparano, J. A.; Wang, M.; Martino, S.; Jones, V.; Perez, E. A.; Saphner, T.; Wolff, A. C.; Sledge, G. W., Jr.; Wood, W. C.; Davidson, N. E. Weekly Paclitaxel in the Adjuvant Treatment of Breast Cancer. *N. Engl. J. Med.* **2008**, *358*, 1663−1671.
(79) Lee, H. J.; Heo, D.-S.; Cho, J.-Y.; Han, S.-W.; Chang, H.-J.; Yi, H.-G.; Kim, T.-E.; Lee, S.-H.; Oh, D.-Y.; Im, S.-A.; Jang, I.-J.; Bang, Y.-J. A Phase I Study of Oral Paclitaxel with a Novel P-glycoprotein Inhibitor, HM30181A, in Patients with Advanced Solid Cancer. *Cancer Res. Treat.* **2014**, *46*, 234−242.
(80) Gelderblom, H.; Verweij, J.; Nooter, K.; Sparreboom, A. Cremophor EL: The Drawbacks and Advantages of Vehicle Selection for Drug Formulation. *Eur. J. Cancer* **2001**, *37*, 1590−1598.
(81) Lee, K.-W.; Lee, K. H.; Zang, D. Y.; Park, Y.; Shin, D. B.; Kim, J. W.; Im, S.-A.; Koh, S. A.; Yu, K.-S.; Cho, J.-Y.; Jung, J.-A.; Bang, Y.-J. Phase I/II Study of Weekly Oraxol for the Second-Line Treatment of Patients with Metastatic or Recurrent Gastric Cancer. *Oncologist* **2015**, *20*, 896−897.
(82) Ma, W. W.; Azad, N. S.; Lam, E. T.; Diamond, J. R.; Dy, G. K.; Opyrchal, M.; Gallagher, D.; Brennen, C.; Cutler, D.; Kramer, D.; Chan, W. K.; Kwan, R.; Fetterly, G. J.; Adjei, A. A.; Jimeno, A. A Phase I Study to Evaluate Safety, Tolerability, Pharmacokinetics and Activity of Oraxol in Patients (pts) with Advanced Malignancies. *J. Clin. Oncol.* **2018**, *36*, 2526.
(83) Clinical trial details can be found at https://www.clinicaltrials.gov/ (accessed 2020-09-12).
(84) Ravi, V.; Wagner, M.; Chen, T. W.; Loong, H. H. F.; Mennel, R. G.; Yen, C.; Clack, G.; Cutler, D.; Kwan, M. R.; Chan, W. K. A Phase II Study of Oraxol in the Treatment of Unresectable Cutaneous Angiosarcoma. *Clin. Oncol.* **2020**, *38*, 11517.
(85) Taxol monograph. *Paclitaxel Injection, USP*; WG Critical Care, LLC. https://www.accessdata.fda.gov/spl/data/0ebbb53f-8a07-4843-bb37-2110e16e1f3e/0ebbb53f-8a07-4843-bb37-2110e16e1f3e.xml (accessed 2020-09-12).
(86) Umanzor, G.; Rugo, H. S.; Barrios, F. J.; Vasallo, R. H.; Chivalan, M. A.; Bejarano, S.; Ramirez, J. R.; Fein, L.; Kowalyszyn, R. D.; Cutler, D. L.; Kramer, D.; Goldfinch, J.; Wang, H.; Moore, T.; Kwan, R. M. F. Oral Paclitaxel with Encequidar (OPE): The First Orally Administered Paclitaxel Shown to be Superior to IV Paclitaxel on Confirmed Response and Survival with Less Neuropathy: A Phase III Clinical Study in Metastatic Breast Cancer. In *Proceedings of the San Antonio Breast Cancer Symposium*, San Antonio, TX, December 10−14, 2019.
(87) The press release can be found here: https://ir.athenex.com/news-releases/news-release-details/athenex-announces-fda-acceptance-filing-us-nda-oral-paclitaxel (accessed 2020-12-04).

https://doi.org/10.1021/acs.jmedchem.0c01826
J. Med. Chem. 2021, 64, 3677−3693